

# NASA CONTRACTOR REPORT



NASA CR-2



TECH LIBRARY KAFB, NM

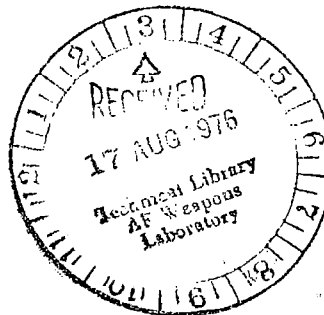
NASA CR-2719


LOAN COPY: RETURN TO  
AFWL TECHNICAL LIBRARY  
KIRTLAND AFB, N. M.

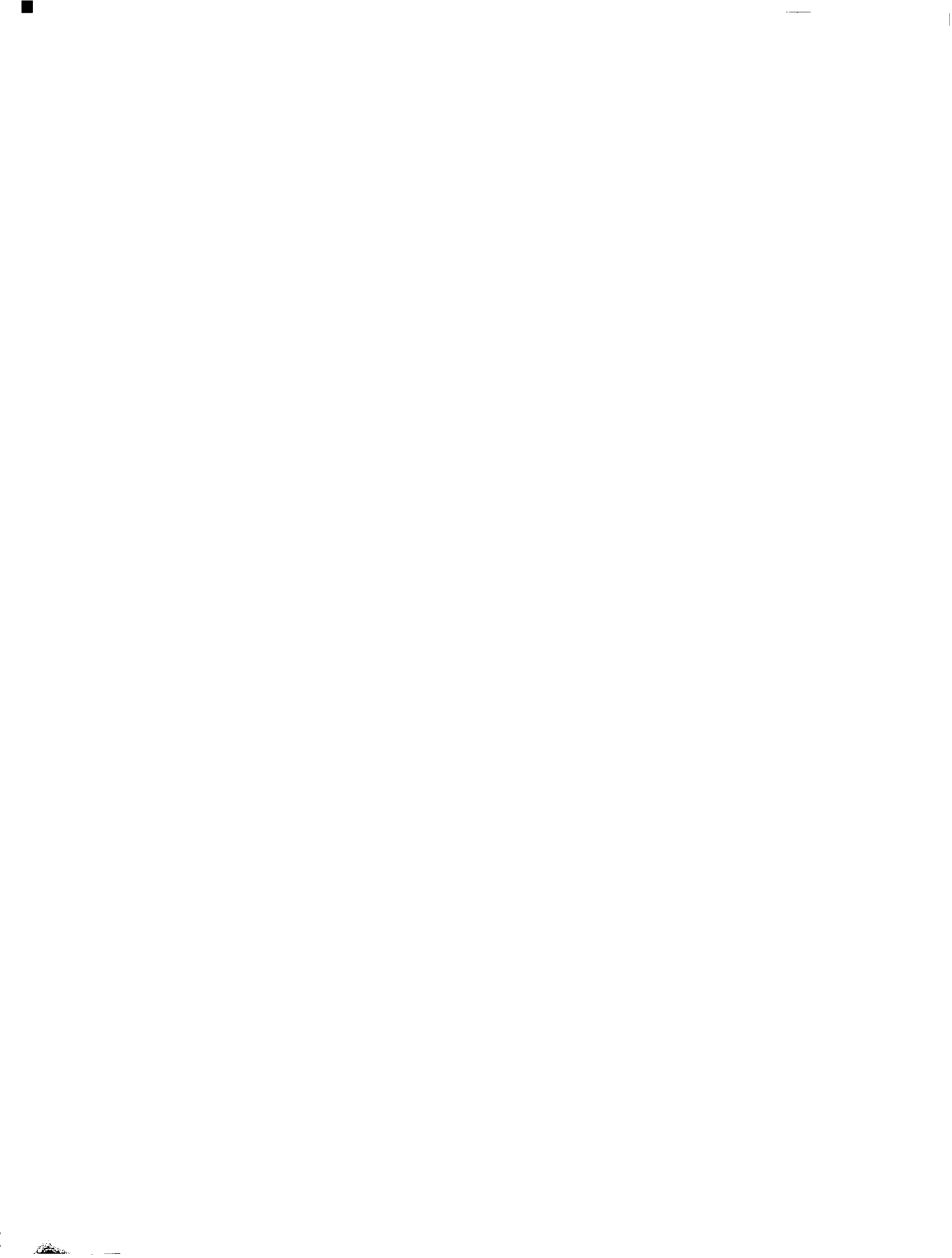
## PLASMA CORE REACTOR SIMULATIONS USING RF URANIUM SEEDED ARGON DISCHARGES

*W. C. Roman*

*Prepared by*  
UNITED TECHNOLOGIES RESEARCH CENTER  
East Hartford, Conn. 06108  
*for Langley Research Center*



1. Report No. NASA CR-2719	2. Government Accession No.	3. Recip  0061442
4. Title and Subtitle PLASMA CORE REACTOR SIMULATIONS USING RF URANIUM SEEDED ARGON DISCHARGES		5. Report Date July 1976
		6. Performing Organization Code
7. Author(s) W. C. ROMAN		8. Performing Organization Report No.
		10. Work Unit No.
9. Performing Organization Name and Address United Technologies Research Center East Hartford, CT 06108		11. Contract or Grant No. NAS1-13291
		13. Type of Report and Period Covered Contractor Report
12. Sponsoring Agency Name and Address National Aeronautics and Space Administration Washington, DC 20546		14. Sponsoring Agency Code
15. Supplementary Notes Project Manager, Frank Hohl, Environmental and Space Sciences Division, NASA Langley Research Center, Hampton, Virginia		
16. Abstract Experimental results are described in which pure uranium hexafluoride was injected into an argon-confined, steady-state, rf-heated plasma to investigate characteristics of plasma core nuclear reactors. 80 kW (13.56 MHz) and 1.2 MW (5.51 MHz) rf induction heater facilities were used to determine a test chamber flow scheme which offered best uranium confinement with minimum wall coating. The cylindrical fused-silica test chamber walls were 5.7-cm-ID by 10-cm-long. Test conditions included rf powers of 2-85 KW, chamber pressures of 1-12 atm, and uranium hexafluoride mass-flow rates of 0.005-0.13 g/s. Successful techniques were developed for fluid-mechanical confinement of rf-heated plasmas with pure uranium hexafluoride injection.		
17. Key Words (Suggested by Author(s)) (STAR category underlined) Gas Core Reactor RF-Heated Uranium Plasma Uranium Plasma Confinement		18. Distribution Statement  Unclassified - Unlimited  Subject Category 73
19. Security Classif. (of this report) Unclassified	20. Security Classif. (of this page) Unclassified	21. No. of Pages 44
		22. Price* \$3.75



CONTENTS

	Page
SUMMARY . . . . .	1
LIST OF SYMBOLS . . . . .	2
INTRODUCTION. . . . .	3
DESCRIPTION OF EQUIPMENT. . . . .	5
RF Induction Heater Facilities . . . . .	5
Test Chamber Flow Configurations . . . . .	5
UF <sub>6</sub> Handling System. . . . .	7
Diagnostics. . . . .	8
Operating Procedures . . . . .	10
DISCUSSION OF RESULTS . . . . .	10
Exploratory Tests. . . . .	10
Follow-on Tests. . . . .	13
REFERENCES. . . . .	15
TABLES I Through IV . . . . .	16
FIGURES 1 Through 23 . . . . .	20

PLASMA CORE REACTOR SIMULATIONS USING  
RF URANIUM SEEDED ARGON DISCHARGES

W. C. Roman  
United Technologies Research Center

SUMMARY

An experimental investigation was conducted using the United Technologies Research Center (UTRC) 80 kW and 1.2 MW rf induction heater facilities to aid in developing the technology necessary for designing a self-critical fissioning uranium plasma core reactor (PCR). Pure uranium hexafluoride ( $UF_6$ ) was injected into argon-confined, steady-state, rf-heated plasmas in uranium plasma confinement tests. The objective was to achieve maximum confinement of uranium vapor within the plasma while simultaneously minimizing the uranium compound wall deposition. In all tests, the plasma was a fluid-mechanically confined vortex-type contained within a fused-silica cylindrical test chamber. Exploratory tests were conducted using the 80 kW rf induction heater ( $f = 13.56$  MHz) with the test chamber at approximately atmospheric pressure and discharge power levels on the order of 10 kW. Four different test chamber flow configurations were tested to permit selection of the configuration offering the best confinement characteristics for subsequent tests at higher pressure and power in the 1.2 MW rf induction heater facility.

The exploratory test configuration selected for use in the more extensive rf plasma tests using the 1.2 MW rf induction heater employed a radial-inflow vortex, driven by injectors located on only one of the water-cooled copper endwalls. In addition to thru-flow ducts located at the center of each endwall, an axial bypass annulus was located near the periphery of the endwall opposite the vortex injectors. A concentric set of water-cooled, fused-silica tubes formed the peripheral wall. The cylindrical test chamber was 5.7-cm-ID by 10-cm-long. This test chamber flow configuration was designed to operate at pressures up to approximately 20 atm and rf discharge power levels up to about 100 kW. In the majority of tests, a single  $UF_6$  injector protruded 2.0 cm into the test chamber; the injector was on the centerline axis located concentrically within the thru-flow duct of one endwall.  $UF_6$  was supplied to the injector from a heated cylinder capable of supplying the gaseous  $UF_6$  at temperatures up to 450 K and pressures up to 20 atm. The rf plasma tests in the 1.2 MW rf induction heater were conducted over a range of test chamber pressures from 1 to 12 atm and rf discharge power levels from 10 to 85 kW. The  $UF_6$  mass flow rate ranged from 0.01 to 0.13 g/s.

Diagnostic measurements included: plasma physical and electrical characteristics; calorimetric power losses; radiation intensity in different wavelength bands with and without injection of  $UF_6$ ; on-axis spectral emission scans between 300-700 nm; side-on absorption measurements using both an argon-ion laser system (514.5 nm) and a cw single-frequency tunable dye laser system (591.5 nm); and, analyses and identification of samples of wall deposits from selected tests using electron diffraction, x-ray diffraction, electron microprobe, and IR spectrophotometer techniques.

The overall test results indicate applicable flow schemes have been developed for fluid mechanical confinement of uranium when pure  $UF_6$  is injected into argon confined, high-temperature, rf-heated plasmas. A typical successful test run had the following operating characteristics:  $UF_6$  flow rate = 0.1 g/s, argon flow rate = 3 g/s, operating pressure = 2 atm, operating discharge power level = 70 kW, total operating time = 10 min, and a total deposition of uranium or uranium compounds on the peripheral wall of 25 mg.

Tests to increase the quantity of uranium confined within the rf-heated plasma, while simultaneously minimizing deposition of the uranium compounds on the peripheral wall of the plasma test chamber combined with additional diagnostic analyses, are in progress.

#### LIST OF SYMBOLS

d	discharge diameter at axial midplane, cm
f	rf operating frequency, MHz
$I/I_0$	transmission, dimensionless
$l$	optical path, cm
$M_i$	mole fraction, dimensionless
$\dot{m}_{Ar}$	argon mass flow rate, g/s
$\dot{m}_{UF_6}$	$UF_6$ mass flow rate, g/s
P	chamber pressure, atm

$Q_D$	total discharge power, kW
$Q_R$	power radiated, kW
T	temperature, deg K
t	time, min
$\Delta\lambda$	wavelength band, nm

## INTRODUCTION

Fissioning uranium plasma core reactors (PCR) could be used as a prime energy source for many space and terrestrial applications. In addition to aerospace propulsion applications, several space power and/or terrestrial options are being considered; these include, direct pumping of lasers, photochemical and thermochemical hydrogen production processes, MHD power conversion, and advanced closed-cycle gas turbine driven electrical generators. Principal features and advantages of these systems include high thermodynamic cycle efficiency, continuous fuel reprocessing, and direct coupling of the radiant energy. Reference 1 discusses the overall status of plasma core reactor technology, the various energy conversion concepts, conceptual designs of various configurations, and a summary of all current research directed toward demonstrating the feasibility of fissioning uranium PCR's.

A principal technology required to establish the feasibility of fissioning uranium plasma core reactors is the fluid mechanical confinement of the hot fissioning uranium plasma with sufficient containment to both sustain nuclear criticality and minimize deposition of uranium or uranium compounds on the confinement chamber peripheral walls. Figure 1 is a sketch of one unit cell configuration of a plasma core reactor. The reactor would consist of one or more such cells imbedded in beryllium oxide and/or heavy-water moderator and surrounded by a pressure vessel. In the central plasma fuel zone, gaseous uranium (injected in the form of  $UF_6$  or other uranium compound) is confined by argon buffer gas injected tangentially at the periphery of the cell. In applications in which it is desired to couple thermal radiation from the fissioning uranium plasma to a separate working fluid, the thermal radiation is transmitted through the argon buffer gas layer and subsequently through internally-cooled transparent walls to a working fluid channel such as shown in figure 1. The mixture of nuclear fuel and argon buffer gas is withdrawn

from one or both endwalls at the axial centerline. For other applications in which it is desired to extract power in the form of nonequilibrium, fission-fragment-induced short wavelength radiation emissions, the transparent wall would be removed and a medium such as lasing gas mixtures would be mixed with either the fissioning uranium fuel or the buffer gas. The reason for this distinction is that most transparent wall materials have intrinsic radiation cutoffs at wavelengths longer than those expected to be emitted in the form of fission-fragment-induced nonequilibrium electromagnetic radiation. Typically, for plasma conditions with an edge-of-fuel-region temperature of approximately 5000 K, operating pressures in the fissioning uranium plasma are on the order of 500 atm. This is dependent upon the combined partial pressures of nuclear fuel required for criticality, dissociation products, electrons from ionized species, and some argon buffer gas present in the fuel region. As part of the planned NASA program to determine the feasibility of plasma core reactors, Los Alamos Scientific Laboratory (LASL) is currently performing cavity reactor experiments which employ gaseous  $UF_6$ .

Plasma core reactor technology studies at UTRC currently consist of several experiments and theoretical investigations directed toward evaluating the feasibility of the PCR concept. Extensive non-nuclear vortex flow and plasma fluid mechanical research has been conducted over the past fifteen years at UTRC.

Previously reported experiments (ref. 2) have been conducted on the confinement of rf plasmas. These tests were directed primarily toward development of a high-intensity, high-power-density plasma energy source (equivalent black-body radiating temperatures  $> 6000$  K). Some of these initial exploratory tests included direct injection of very dilute mixtures of  $UF_6$  (typically, 1%  $UF_6$  in an argon carrier-gas) into the rf-argon plasma. Coating of the fused-silica peripheral wall occurred but sustained plasma operation for several minutes was demonstrated. Particle feeder systems were also developed which permitted steady-state injection of C, W,  $UO_2$ , and  $U_3O_8$  into test chambers operating at pressures up to 40 atm. In general, these test results confirmed that high simulated fuel concentrations could be confined fluid-mechanically with steep concentration gradients at the edge-of-fuel location.

The objective of this paper is to present some recent results of the Plasma Core Reactor (PCR) simulation tests conducted at UTRC using pure  $UF_6$  injected into steady-state, argon-confined, rf-heated plasmas.



## DESCRIPTION OF EQUIPMENT

### RF Induction Heater Facilities

The experiments were conducted using both an 80 kW and a 1.2 MW rf induction heater systems. The 80 kW facility was used in the initial set of exploratory tests. Figure 2 is a schematic diagram of the 80 kW rf induction heater electrical system. A photograph of an assembled exploratory test configuration installed under the  $2\frac{1}{2}$ -turn, 7.5-cm-dia water-cooled rf work coil ( $0.7 \mu\text{H}$ ) of the 80 kW facility is shown in figure 3. The easily modified work coil is connected to the output of the power amplifier by means of a tunable  $\pi$ -coupling network (see fig. 2). The initial system was modified to operate at 13.56 MHz and low-speed motor drives were installed on the plate and load tuning capacitors to aid in efficiently coupling rf power into plasmas having a relatively wide range of sizes and impedances.

A photograph of the assembled follow-on test configuration installed under the set of 9-cm-dia water-cooled rf work coils within the resonator section of the 1.2 MW rf induction heater is shown in figure 4. Part of the 1.2 MW rf induction heater assembly is shown in figure 4. Figure 5 is a block diagram of the 1.2 MW rf induction heater electrical system. The 1.2 MW rf induction heater was operated at approximately 5.5 MHz. All stages of the 1.2 MW rf system contained controls for tuning the matching circuit at the final power amplifier input, thus aiding in increasing the overall system efficiency. The rf output is supplied by two power amplifier tubes (440 kW output each) which drive a resonant tank circuit of unique design. The output of the two amplifiers is coupled by a push-pull resonator (all stages operated in class C). The entire resonator section consists of two arrays of ten vacuum capacitors, located (as shown in figs. 4 and 5) within a 1.7-m-dia cylindrical aluminum test tank. The front of the test tank is a removable dome (shown removed in fig. 4) containing five windows for observation and/or diagnostic equipment access. A complete description of the rf heater facility is presented in reference 2.

### Test Chamber Flow Configurations

Figure 6 contains schematic diagrams of the various test chamber flow configurations employed in the exploratory tests conducted in the 80 kW rf facility. Different configurations were tested to permit selection of the flow geometry with the best confinement characteristics. A gas-cooled 5.7-cm-ID x 6.1-cm-OD fused-silica tube formed the peripheral boundary of the test

chamber. A symmetrically-arranged set of water-cooled endwalls spaced 10 cm apart formed the axial boundary of the test chamber. Argon was injected through a set of 1.7-mm-ID vortex injectors equally-spaced around the periphery of one or both endwalls to provide the confining flow. As shown in figure 6(d), some tests were conducted with the argon gas injected tangentially through hypo-sized injectors located within the fused-silica peripheral wall. The exhaust gases were removed through one or both endwalls with thru-flow ducts on the centerline and/or off-axis annular exhaust ducts. To permit steady-state injection of pure  $UF_6$  into the plasma, several types of concentric-tube, water-cooled copper injectors were fabricated and located concentrically within the on-axis thru-flow duct.  $UF_6$  was selected as the form of uranium bearing compound for injection into the plasma because it could be supplied in a gaseous form. Earlier tests in previous programs had indicated that injection of uranium in the form of small particulates was a more difficult technology. However,  $UF_6$  is very reactive chemically and must be heated to be sure that it remains in the gaseous state and does not condense on the injector walls prior to entering the plasma test chamber. Therefore special cleaning procedures, operating procedures, and heating and feeding techniques had to be employed. These included the use of steam augmentation and electrical heater assemblies throughout the  $UF_6$  injector and feed systems to eliminate the possible condensation and subsequent plugging of the  $UF_6$  feeder lines. As shown in figures 6(a) and 6(d), the  $UF_6$  injector could be extended into the test chamber/plasma region to eliminate some of the end effects. The various test chamber flow geometries and combinations thereof, permitted a wide variation in the types of flow conditions obtainable with  $UF_6$  injection. Based on the exploratory test results, the test chamber flow configuration shown in figure 6(a) was selected for the continued tests employing the 1.2 MW rf induction heater system. This geometry has several attractive features: ability to vary the distribution of exhaust gas flow (axial bypass); ease of change in the injection area of the argon vortex injectors; and, ease of change in the location of the on-axis  $UF_6$  injector.

Figure 7 is a sketch of the test chamber configuration employed in the 1.2 MW rf induction heater using pure  $UF_6$  injection. For simplicity, only half the chamber is shown. As in the exploratory tests, the axial length between endwalls was 10 cm. Because of the higher power, higher pressure, and associated radiation levels involved, a concentric set of water-cooled fused-silica tubes were used as the peripheral wall. The inner tube was 5.7-cm-ID x 6.1-cm-OD; the outer tube was 6.5-cm-ID x 7.3-cm-OD. An alternate outer fused-silica tube was also prepared, having a 9-mm wall thickness (see fig. 7) to permit safe operation, if required, at relatively high chamber pressures ( $\approx 40$  atm). The water-cooled copper endwalls incorporate provisions for driving the vortex from one (or symmetrically from both) endwalls. The other endwall (not shown in fig. 7) has provision for removing the exhaust gas

through an axial bypass on the periphery of the endwall. Both endwalls have the option for removing varying amounts of the exhaust gas through the on-axis thru-flow ducts. As shown in figure 7, the  $\text{UF}_6$  injector, located on-axis and concentrically within the right endwall, was fabricated from a 50-cm-long three concentric copper tube assembly. In the majority of tests, the injector tip extended 2 cm into the test chamber. High pressure water (20 atm) heated to approximately 350 K via a steam heat exchanger flowed at 0.14 l/s between the concentric tubes of the  $\text{UF}_6$  injector. This provided cooling relative to the hot plasma environment while still maintaining a high enough temperature in the injector to permit flow of the pressurized gaseous  $\text{UF}_6$  without solidification and subsequent plugging in the  $\text{UF}_6$  transfer line.

### $\text{UF}_6$ Handling System

In support of the rf plasma experiments, a  $\text{UF}_6$  handling and feeder system to provide a controlled and steady flow of heated  $\text{UF}_6$  at temperatures up to 500 K was developed. Figure 8 is a schematic diagram of the  $\text{UF}_6$  system. The system was designed to provide  $\text{UF}_6$  mass flow rates up to about 5 g/s and subsequent possible injection of  $\text{UF}_6$  into test chambers operating at pressures up to 20 atm. Figure 9 shows the vapor pressure curve for  $\text{UF}_6$  for the operating ranges of interest. The principal components of the system are the  $\text{UF}_6$  boiler, the boiler heat supply system, and the  $\text{UF}_6$  condenser (exhaust) system. The boiler is a 2 l monel cylinder rated at 200 atm working pressure. monel was selected because of its resistance to chemical attack by hot, pressurized  $\text{UF}_6$ . A heat exchanger to provide internal heating is located in the bottom of the boiler and thermocouples are located at both the top and bottom of the boiler. The thermocouple wells, heat exchangers, and  $\text{UF}_6$  flow lines were all fabricated from 6.4-mm-OD monel tubing. A 3.5 kW electrical heater surrounds the boiler and is used to reach the desired equilibrium temperature and pressure prior to flowing the  $\text{UF}_6$ . In the tests reported herein, use of the electrical heater assembly alone was sufficient to provide the required flow rates; in future tests employing higher  $\text{UF}_6$  flow rates for longer time periods, electrically-heated gaseous  $\text{N}_2$  can be supplied to the  $\text{UF}_6$  boiler heat exchanger. Control on the rate of  $\text{UF}_6$  evaporation is accomplished by using a bypass loop, as shown in figure 8. During operation of the system, the gaseous  $\text{UF}_6$  flows from the boiler through a metering valve and a linear mass flow meter (calibrated for  $\text{UF}_6$  operation) prior to entering the  $\text{UF}_6$  injector located within the rf plasma test chamber. The exhaust from the test chamber, comprised of argon,  $\text{UF}_6$  and other volatile uranium compounds is collected in the  $\text{UF}_6$  condenser system located downstream of the test chamber. The condenser system consists of two 0.5 l stainless-steel tanks (connected in parallel) immersed in liquid  $\text{N}_2$ . All valves throughout the system are welded-bellows type. A neutralizing trap ( $\text{NaOH} + \text{H}_2\text{O}$ ) is located downstream

of the condenser system to remove any residual uranium or uranium compounds which pass through the flow trap, shown in figure 8. To provide additional safety, a high flow capacity exhaust vent and gas scrubber system is installed on the Laboratory roof above the test apparatus.

### Diagnostics

The total power deposited into the plasma was obtained from an overall test chamber heat balance by summing the power lost by radiation, power deposited into the annular coolant of the peripheral wall, power deposited into the endwall assemblies, power convected out the exhaust ducts, as well as, power deposited into the effluent gas heat exchanger and  $UF_6$  injector assemblies.

The power radiated from the plasma was measured using a radiometer and chopper wheel assembly. A thermopile detector with a quartz window was used as the radiometer sensing element. Its output was connected to an operational amplifier and displayed on a strip chart recorder. Radiation within different wavelength bands was measured using various filters. The response of the thermopile with filters was calibrated using a standard source of spectral irradiance. The total power radiated from the plasma and in each wavelength band was calculated assuming isotropic radiation including allowance for blockage due to the rf work coils.

The physical size and shape of the plasma was determined from photographs taken using various neutral density filters. Continuous observation of the plasma was accomplished using a lens-projection-screen system. During all tests, the voltage, current and power of various stages of the rf systems, were monitored by meters. In addition, strip chart recorders were also used to continuously monitor the rf plate voltage, plate current, and resonator voltage.

Figure 10 is a schematic of the diagnostic systems used in the exploratory rf plasma tests. A 0.25-m monochromator and a S-20 response photomultiplier detector were used to obtain spectral emission data between 300-700 nm. Twenty-five  $\mu\text{m}$ -wide entrance and exit slits were employed. These measurements were taken on-axis at the midplane of the test chamber. The scanning rate was 100 nm/min and the data were recorded on a strip chart recorder; measurements were obtained for both argon only and argon plus  $UF_6$  plasmas.

Measurements also included side-on absorption measurements using a cw, single-frequency, tunable dye laser system. The feasibility of this technique was investigated as a possible means for determining the number density and spatial distribution of uranium vapor contained within the discharge boundary in future  $UF_6$ /rf plasma tests containing uranium vapor of heavy concentrations. A argon-ion laser (10 W) was used for the pump power and was operated at 514.5 nm. The unit was used with a methanol and water solution containing rhodamine 6G dye. Rhodamine 6G absorbs in the band 480-530 nm and provides laser gain from 540 to 630 nm. This particular Model dye laser system permits synchronizing the three possible tuning mechanisms: cavity length, etalon length, and cavity prism. The unit employed a single high-finesse, low-loss piezo-scanned tunable etalon, automatic scanning electronics, a low f-m jitter dye circulation system, and a temperature-controlled oven assembly to aid in stability. For high resolution scans, the cavity length is tuned while the etalon is tracked in synchronism with the cavity scan. For large bandwidth scans, the etalon is scanned while the cavity length tracks. The cavity prism is tracked in synchronism with the etalon to keep the laser power constant. For the majority of the exploratory tests reported herein, 1 W of pump power was used. Typical dye laser output powers (narrow line operation at 591.5 nm) were 100 mW. As shown in figure 10, a hollow-cathode uranium lamp was used to select the reference uranium line (591.5 nm) used in these tests. A Fabry-Perot spectrum analyzer was used to define and calibrate the tuning frequency spectrum. A 0.5-m spectrometer with a photomultiplier was used in conjunction with a set of beam splitters and two front surface mirrors, as shown in figure 10. The laser beam ( $\approx 1.5$ -mm-dia) traversed the test chamber on the major axis at a distance 1 cm away from the tip of the  $UF_6$  injector. In these tests the  $UF_6$  injector extended 1 cm into the test chamber. This position was selected since prior rf plasma tests (argon only) included chordal scans at this location from which temperature profiles were determined.

$UF_6$ /rf plasma tests conducted in the 1.2 MW induction heater facility did not include the dye laser system, but the argon-ion laser system operating at 514.5 nm was used for additional side-on absorption measurements taken on-axis at the axial midplane of the test chamber. The test setup was similar to that shown in figure 10.

To permit a detailed analysis of the quantity and composition of the wall deposition incurred after several selected  $UF_6$ /rf plasma tests, samples of the wall residue were collected and analyzed by means of electron diffraction, x-ray diffraction, electron microprobe, and IR spectrophotometric techniques.

## Operating Procedures

In general, the tests (80 kW and 1.2 MW) were first conducted with only argon injected into the test chamber. After sufficient time to establish equilibrium, pure  $UF_6$  was injected for various time periods. Normally, a series of  $UF_6$  tests were conducted with the same fused-silica tube prior to shutdown for post-test examination. In all tests the discharge was ignited using a vacuum start technique at a chamber pressure of approximately 10 mm Hg. This technique had the advantage of eliminating the introduction of foreign materials into the test chamber which would be present with dc arc rod starting techniques and also, in conjunction with the argon feed and the exhaust trap system, permitted a partial purge between tests.

## DISCUSSION OF RESULTS

### Exploratory Tests

TABLE I is a summary of the exploratory tests conducted, including a brief description of the test chamber configuration and flow control scheme, range of test conditions, number of tests conducted, and pertinent comments applicable to each. A direct one-to-one comparison between each of the various configurations was difficult because of the different operating characteristics associated with each test. Also, due to time and cost constraints, each configuration by no means represents the optimum in design and sizing of the various components.

Based on the overall test results, the test chamber flow configuration shown in figure 6(a) was selected as the one best-suited for use in the follow-on rf plasma tests employing the 1.2 MW rf induction heater system. With this configuration, a relative maximum mass flow rate of pure  $UF_6$  (0.04 g/s) injected directly into the argon plasma was achieved with corresponding minimum wall coating, thus offering potentially the best confinement characteristics. In addition, this test chamber flow configuration possesses significant flexibility in the control of the flow field and exhaust gas distribution.

To illustrate the effect of the pure  $UF_6$  injection on the plasma discharge, figure 11 shows the operating conditions and results of corresponding radiation measurements for a typical exploratory test. In the majority of tests, attempts were made to maintain constant as many of the independent variables as possible during the injection of  $UF_6$ . However, changes in the

rf power and/or tuning and associated flow rates were sometimes required to prevent discharge extinguishment or plasma oscillations. In general, the introduction of pure  $UF_6$  into the discharge significantly altered the impedance of the plasma which, in turn, determined the plasma size and electrical conductivity. This was manifested principally as a significant increase in the radiation emitted from the plasma; correspondingly, a moderate increase in the total power deposited into the plasma was also observed. The table and bar graph of figure 11 illustrates both these effects. Note that a significant amount of the increase in radiation occurred in the visible and near-UV wavelength bands. At the relatively low discharge power and pressure levels of these exploratory tests, the discharge was quite sensitive to changes in both the argon mass flow rate and the  $UF_6$  mass flow rate. Occasionally, when the  $UF_6$  injection mass flow rate exceeded a certain level, corresponding to a given set of test conditions, distortion occurred (plasma unsteadiness) in the central region of the plasma; this was sometimes followed by extinguishment of the discharge.

Periodically throughout the exploratory rf plasma tests, spectral emission measurements throughout the wavelength band from 300-700 nm were taken on-axis at the axial midplane using the 0.25-m monochromator system shown in figure 10. Figure 12 illustrates some results obtained for the wavelength band between 400 to 460 nm. Many of the strong argon, uranium, and fluorine lines present in the wavelength range from 300-700 nm have been identified, cataloged, and compared with those documented in the literature. Also to aid in the analyses of the present and future tests,  $UF_6$  equilibrium composition data were calculated for total pressures from  $10^{-4}$  to 1 atm and over a range of temperatures from 300 to 10,000 K. Figure 13 is an example of this  $UF_6$  equilibrium composition data. For all practical purposes, at a pressure of approximately 1 atm complete thermal decomposition of  $UF_6$  has occurred at a temperature of about 4700 K.

To demonstrate the feasibility and practicality of using a cw single-frequency tunable dye laser system for making uranium plasma absorption measurements, several tests were conducted using the dye laser system illustrated in figure 10. Significant effort had to be devoted to properly shielding the entire dye laser and associated diagnostic equipment from the rf fields. As shown in figure 10, the dye laser beam traversed the test chamber on the major axis at a distance of 1 cm away from the tip of the  $UF_6$  injector. Based on prior spectral emission chordal scans taken under similar test conditions (argon only), the temperature profiles determined (based on both absolute line and continuum radiation) indicated centerline temperatures of approximately 8000 K exist with a slight off-axis peak at a radius ratio of about 0.5.

Figure 14 shows an example of the absorption measurements obtained from the actual strip chart recorder output in the exploratory rf plasma experiments with pure  $UF_6$  injection. The 591.54 nm uranium line was selected as it is a relatively strong uranium I line and appeared well-defined in the earlier spectral emission scans. The lower state for the 591.54 nm line is the uranium I ground state. The half-width of the laser line at the 591.54 nm wavelength was approximately  $10^{-4}$  nm. To obtain the measurements shown in figure 14, the scanning generator of the dye laser system was activated to an automatic continuous scan mode as shown by the output data in the left portion of figure 14. Only argon was present in the rf plasma discharge during these initial scans. The 8 GHz range (free spectral range of the confocal Fabry-Perot spectrum analyzer) translates to approximately  $10^{-2}$  nm on the wavelength scale. Many such scans at different operating test conditions were completed with only several (at fixed test conditions) shown in figure 14 for simplicity. The test conditions for the argon-only case were similar to those shown in the table in figure 11. The zero reference line (zero transmission) is shown at the top of figure 14. As noted, no absorption was detected for any of the argon-only test conditions. When pure  $UF_6$  was injected into the discharge, sufficient time was allowed for all conditions to come to equilibrium ( $\approx 10$  seconds); additional scans were then completed. Results from tests at two different  $UF_6$  mass flow rates are shown at the right of figure 14. The first case corresponds to a  $UF_6$  mass flow rate of approximately 0.02 g/s. The measurements indicate an absorption of approximately 25% (corresponding to an  $I/I_0 = 0.75$ ). Doubling the mass flow rate of  $UF_6$  to approximately 0.04 g/s increased the relative absorption to about 55% ( $I/I_0 = 0.45$ ) for the second case. Based on an assumed 50-50 occupancy (ground state/excited state), a temperature of 8000 K, an optical path length of 2 cm (relatively small core due to close proximity of the  $UF_6$  injector), and including a factor for ionization reduction, the ground state uranium I atom number density based on the absorption measurements were estimated to be approximately  $8 \times 10^{12}$  atoms/cm<sup>3</sup> and  $2 \times 10^{13}$  atoms/cm<sup>3</sup>, respectively, for the two cases. This compares with approximately  $10^{14}$  atoms/cm<sup>3</sup> based on temperature and pressure calculations. These results are encouraging and demonstrated that a dye laser system combined with optical scanning and tracking may be employed in future rf plasma  $UF_6$  confinement tests to permit mapping of the spatial absorption distribution; from this and other measurements the total number density and spatial distribution of uranium vapor contained both within the discharge boundary and in trace quantities in the buffer layer may be determined.

Periodically throughout the exploratory test series, portions of the fused-silica peripheral tubes were examined for thermal stresses and wall deposition. Figure 15 is a photograph of two of the tubes used in the exploratory tests with pure  $UF_6$  injection. The analysis indicated some degree of thermal stress was present in the central region of the fused-silica



tube, generally following the outline of the rf work coil. This was as expected due to the limited air jet cooling supplied to the fused-silica tube and the close proximity of the rf plasma to the wall during the majority of tests. The fused-silica tube numbered 8 in figure 15 is representative of the type of wall coating obtained after about two minutes of operation in the relatively high  $UF_6$  mass flow rate range.

#### Follow-on Tests

TABLE II is a summary of the tests conducted in the 1.2 MW rf induction heater using the test chamber flow configuration shown in figure 7. Over 140 tests were conducted over the range of test conditions shown in TABLE II. The pure  $UF_6$  was injected on-axis from one endwall. Results similar to those shown in figure 11 were obtained and additional spectral measurements in the 300-700 nm range were taken. The effect of the 2-mm-thick passage of annular water coolant was noted in the upper wavelength cutoff of about 1300 nm as compared to the exploratory tests which employed only gas cooling. In general, the higher power, higher pressure argon rf plasma discharge employed in the 1.2 MW rf induction heater tests was less susceptible to perturbations due to the injection of pure  $UF_6$ . Thus, a greater mass flow rate of  $UF_6$  could be injected while still maintaining a well-confined, stable discharge. Occasionally, under certain extreme combinations of test conditions, indications of plasma unsteadiness were also observed to occur.

The maximum mass flow rate of pure  $UF_6$  employed was 0.13 g/s. This corresponded to a chamber pressure of 1.7 atm, argon plasma power level of 71 kW, argon buffer gas mass flow rate of 3.2 g/s. The test at maximum  $UF_6$  flow rate extended over a time interval of ten minutes.

During the latter part of the tests using the 1.2 MW rf induction heater, ten tubes were selected for analysis of wall deposits by several techniques, including electron diffraction, x-ray diffraction, electron microprobe, and IR spectrophotometry. TABLE III is a summary of the results and shows the types of compounds deposited on the peripheral wall. To assist in analyzing the wall deposition samples, a detailed cataloging of the possible uranium compounds that may form with the associated diffraction pattern lines and physical characteristics was also completed and is shown in TABLE IV. Figure 16 is a photograph showing four of the ten tubes which were analyzed. Only one complete test was conducted prior to the removal of these tubes from the test section. Note that greater than an order of magnitude reduction in the deposition of uranium compounds was achieved in these tests. It should be pointed out that a relatively uniform deposition of approximately 19 mg is difficult to detect visually. The  $SiO_2$  detected using the IR

spectrophotometer, was believed to be from the fused-silica tube itself and partly due to the silicone grease used in the O-rings for sealing the fused-silica tube to the endwall assembly. The agreement between the different analysis techniques is reasonable considering the statistical nature of sampling the residue and partial exposure to the atmosphere in the preparation of the small samples. In addition to the results shown in TABLE III for the fused-silica peripheral tube, some  $UF_4$  was found to be present on the surface of the endwalls,  $UF_6$  injector, and within the exhaust thru-flow duct. Figures 17 through 21 show examples of the results obtained from the various analysis techniques. Figure 17 illustrates the type of electron diffraction patterns obtained. For the particular sample shown, the primary compound was  $UO_2$  with a trace amount of  $UF_4$ . The tabular data to the right of the actual diffraction pattern photograph gives additional details on the compounds characteristics. Photomicrographs of the residue wall coating (800X magnification) and corresponding to the three principal color samples analyzed are shown in figure 18. The distinctly different crystalline structure of each is clearly evident in the photographs. Figure 19 contains four photographs showing the different x-ray diffraction patterns obtained from post-test analysis of the fused-silica tube residue. In all cases, the samples were subjected to copper  $K_{\alpha}$  radiation in a Debye camera. In addition to the three color powders obtained (black, rust, green), a black chip sample was also included for comparison. The distinctly different x-ray diffraction patterns from each sample is evident from the photographs. Figure 20 contains three photographs of the distribution of U, F, and O from samples of the black powder residue wall coating from a post-test x-ray analysis. The magnification was approximately 350X. Figure 21 is an example of the recorder output trace obtained from the IR spectrophotometry absorption measurements of a post-test analysis of the residue wall coating. At the bottom of the trace is noted the particular compounds associated with the peaks.

Figure 22 shows an example of some of the absorption measurements obtained in the 1.2 MW rf plasma experiments with pure  $UF_6$  injection. Refer to figure 10 for the basic diagnostic setup. In these tests, an argon-ion laser beam of approximately 300 mW power and operating at 514.5 nm was used. Figure 22 shows the change in transmission ( $I/I_0$ ) which occurred for various changes in the  $UF_6$  mass flow rate. A semi-log plot was used to give an indication of the possible exponential dependence of the transmission on the  $UF_6$  mass flow rate. In this case the  $UF_6$  mass flow rate would be related to the concentration. The product of absorption coefficient, concentration, and optical path length forms the exponent in the relationship with transmission. Post-test calibration indicated the transmission returned to approximately the initial value, thus confirming the observation of minimum wall coating. Figure 23 is a photograph showing the rf plasma with pure  $UF_6$  injection within the 1.2 MW rf induction heater.

The test results indicate successful techniques have been developed for fluid mechanical confinement of uranium in argon-confined high-temperature, high-pressure, rf-heated plasmas with pure UF<sub>6</sub> injection. Included, has been the development of the associated handling and feeder techniques for steady-state injection of pure UF<sub>6</sub> into the rf plasma discharge. Various diagnostic techniques have also been developed and applied to determine some of the uranium plasma characteristics and composition of the uranium compound wall deposition.

Continuing tests to further increase the quantity of uranium confined within the rf-heated argon plasma, while simultaneously minimizing deposition of the uranium compounds on the peripheral walls of the plasma test chamber, are in progress. Included is the development and application of x-ray absorption methods for determining contained uranium mass.

#### REFERENCES

1. Latham, T. S., F. R. Biancardi, and R. J. Rodgers: Applications of Plasma Core Reactors to Terrestrial Energy Systems. AIAA Paper 74-1074, AIAA/SAE 10th Propulsion Conference, San Diego, California, October 21-23, 1974.
2. Roman, W. C., and J. F. Jaminet: Development of RF Plasma Simulations of In-Reactor Tests of Small Models of the Nuclear Light Bulb Fuel Region. United Aircraft Research Laboratories Report L-910900-12, Prepared Under Contract SNPC-70, September 1972. Also issued as NASA CR-129299.

TABLE I

SUMMARY OF EXPLORATORY TESTS CONDUCTED IN 80-kW RF INDUCTION HEATER  
USING ARGON BUFFER GAS AND PURE UF<sub>6</sub> INJECTION

Test Chamber 5.7-cm-ID x 10-cm-long  
On-axis UF<sub>6</sub> injection (flush to 3 cm into chamber)

Test Chamber Configuration and Flow Control Scheme	Range of Test Conditions (all tests conducted at operating frequency of 13.56 MHz)	Tests	Comments
Single endwall driven vortex injection. Combination of on-axis thru-flow (both ends) and single axial bypass exhaust.* See Fig. 4a.	Argon mass flow rate 0.15-1.5 g/s UF <sub>6</sub> mass flow rate 0.005-0.040 g/s Chamber pressure 1-1.2 atm Axial bypass flow - 0-100% On-axis thru-flow - 0-100% RF discharge power 2-15 kW Discharge diameter 3.8-5.5 cm	16	Relatively high UF <sub>6</sub> flow rates obtained with light coating on central region of peripheral wall. Well confined, stable discharge over wide range of test conditions.
Coaxial flow endwall argon injection, bluff body stabilization. Combination of on-axis thru-flow (both ends) and single axial bypass exhaust. See Fig. 4b.	Argon mass flow rate 0.010-2.1 g/s UF <sub>6</sub> mass flow rate 0.005-0.03 g/s Chamber pressure 1 atm Axial bypass flow 0-100% On-axis thru-flow 0-100% RF discharge power 2-11 kW Discharge diameter 4.5-5.5 cm	8	Central region and extremities of peripheral wall became heavily coated in all tests. Ellipsoidally-shaped dis- charge extending close to peripheral wall. Discharge sensitive to changes in argon/UF <sub>6</sub> mass flow rate. Difficult to tune rf load during UF <sub>6</sub> injection.
Symmetrical endwall driven vortex injection. No on-axis thru-flow. Symmetrical large radius exhaust annuli. See Fig. 4c.	Argon mass flow rate 0.10-1.5 g/s UF <sub>6</sub> mass flow rate 0.005-0.035 g/s Chamber pressure 1 atm RF discharge power 2-15 kW Discharge diameter 4-5.5 cm	10	Central region became moderately coated in all tests. Discharge sensitive to changes in argon/UF <sub>6</sub> mass flow rate. Retuning load required during UF <sub>6</sub> injection to eliminate extinguishment. Occasional discharge oscillation noted.
Peripheral wall driven vortex injection** (endwall augmentation used in some tests). See Fig. 4d.	Argon mass flow rate 0.08-0.2 g/s UF <sub>6</sub> mass flow rate 0.005-0.03 g/s Chamber pressure 1 atm Axial bypass flow 0-100% On-axis thru-flow 0-100% RF discharge power 2-8 kW Discharge diameter 4.5-5.5 cm	5	Entire peripheral wall became heavily coated. Apparent turbulence noted along discharge boundary. Flow control limited due to fixed vortex injector area. Excessive heating of peripheral wall occurred.

\*Test configuration and flow control scheme selected for follow-on tests in 1.2 MW rf induction heater system.

\*\*The peripheral wall injection flow control scheme was used with both the first and third test chamber configurations.

TABLE II

SUMMARY OF RF PLASMA TESTS CONDUCTED IN 1.2 MW RF INDUCTION  
HEATER USING ARGON BUFFER GAS AND PURE UF<sub>6</sub> INJECTION

See Fig.7 for Sketch of Test Configuration  
On-Axis UF<sub>6</sub> Injection from One Endwall Only

Test Chamber Configuration and Flow Control Scheme	Range of Test Conditions	No. of Tests
Dual Endwall Driven Vortex Injection On-Axis Thru-Flow (Both Endwalls) No Axial Bypass	Argon Mass Flow Rate            1.8 - 3.4    g/s On-Axis Thru-Flow Through One Endwall            0 - 25       % RF Discharge Power                20 - 60      kW Range of RF Operating Frequency 5.4700 - 5.5000 MHz Discharge Diameter                2.5 - 3.1    cm Chamber Pressure                    2 - 12       atm UF <sub>6</sub> Mass Flow Rate                0.008 - 0.13 g/s Test Time                              0.17 - 10    min	86
Single Endwall Driven Vortex Injection On-Axis Thru-Flow (One Endwall Only Opposite Vortex Drive) Single Axial Bypass (Endwall Opposite Vortex Drive)	Argon Mass Flow Rate            2.2 - 3.85   g/s Axial Bypass Flow                    0 - 52       % RF Discharge Power                30 - 85      kW Range of RF Operating Frequency 5.4778 - 5.4878 MHz Discharge Diameter                2.3 - 3.3    cm Chamber Pressure                    1.7 - 5       atm UF <sub>6</sub> Mass Flow Rate                0.013 - 0.131 g/s Test Time                              0.25 - 10    min	57

TABLE III

SUMMARY OF ANALYSIS OF RESIDUE SAMPLES TAKEN FROM INSIDE OF FUSED-SILICA TUBES  
AFTER RF PLASMA TESTS WITH PURE  $UF_6$  INJECTION

Total of 10 Tubes Analyzed  
See Fig. 16 For Photograph Showing Examples of Wall Coating

Analysis Technique	Primary Compound or Element Present in Residue Sample		
	Green Color Sample	Rust Color Sample	Black Color Sample
Electron Diffraction	$UF_4$	$UF_4$	$U_3O_8$ , $UO_2$ , $U_4O_9$
X-Ray Diffraction	$UF_4$	$UO_2$ , $U_4O_9$	$U_3O_8$ , $\alpha UO_3$ (Hexagonal)
Electron Microprobe	U, F, Trace amount of O	U, O, F	U, O, F
IR Spectrophotometry	$UF_4$ , $UO_2F_2$ , $SiO_2$	$UO_2F_2$ , $SiO_2$ , $UO_2$	$UO_2$ , $SiO_2$

TABLE IV

CATALOGED LIST OF (EIGHT) STRONGEST LINES OF POSSIBLE  
 REACTANTS/COMPOUNDS AND ASSOCIATED LINE SPACINGS

Data Taken From American Society of Testing Materials X-ray Card File

Compound	ASTM X-ray Card File No.	d-spacing, Å							
U	11-628	2.93	2.56	2.52	2.48	2.28	1.78	1.53	
UO	17-659	2.83	2.46	1.74	1.48	1.42			
UO <sub>2</sub>	5-0550	3.157	2.735	1.934	1.649	1.579			
αUO <sub>3</sub>	12-43	4.17	3.44	2.65	1.98	1.78	1.71	1.58	1.32
UO <sub>3</sub>	15-201	4.98	3.45	3.26	(Also documented is 18-1429; 4.13, 3.46, 3.29)				
αU <sub>3</sub> O <sub>8</sub>	8-244	4.10	3.37	2.61	2.21	1.95	1.76	1.69	1.56
U <sub>3</sub> O <sub>8</sub>	23-1460	4.15	3.53	2.60	(also documented 23-1345; 4.15, 3.53, 2.60)				
U <sub>4</sub> O <sub>9</sub>	20-1344	3.14	2.721	1.92	1.64	1.248	1.047	0.919	
UF <sub>3</sub>	9-339	3.67	3.58	3.21	2.06	2.02	1.80	1.74	1.44
UF <sub>4</sub>	12-701	7.52	6.63	4.21	4.18	3.95	3.72	3.55	3.29
UF <sub>5</sub>	4-447	5.66	4.68	3.62	3.61	2.44	2.35	2.08	1.96
UF <sub>6</sub>	9-166	5.20	4.51	4.34	4.10	3.80	3.22	2.67	2.56
U <sub>2</sub> F <sub>9</sub>	4-860	4.15	3.42	1.98	1.79	1.65	1.45	1.40	1.37
UO <sub>2</sub> F <sub>2</sub>	4-833	5.22	3.53	3.29	2.09	1.94	1.80	1.63	1.37
*UO <sub>2</sub> F <sub>2</sub>	4-230	5.18	3.51	3.21	2.60	2.10	1.95	1.80	1.78
UC	9-214	2.87	2.47	1.75	1.49	1.43	1.13	1.11	1.01
UC <sub>2</sub>	6-372	3.04	2.98	2.49	1.91	1.77	1.73	1.53	1.24
U <sub>2</sub> C <sub>3</sub>	6-709	3.29	2.85	2.55	1.58	1.47	1.09	1.07	1.02
UN	11-315	2.81	2.44	1.72	1.47	1.12	1.09	0.99	0.94
UN <sub>2</sub>	10-93	3.02	2.62	1.86	1.59	1.22	1.19	1.02	0.89
U <sub>2</sub> N <sub>3</sub>	15-426	4.34	3.08	2.66	1.88	1.61	1.53	1.22	1.19
CU	4-0836	2.08	1.87	1.27	1.09	1.04	0.90	0.85	0.81

α - Hexagonal

\* - Rhombohedral

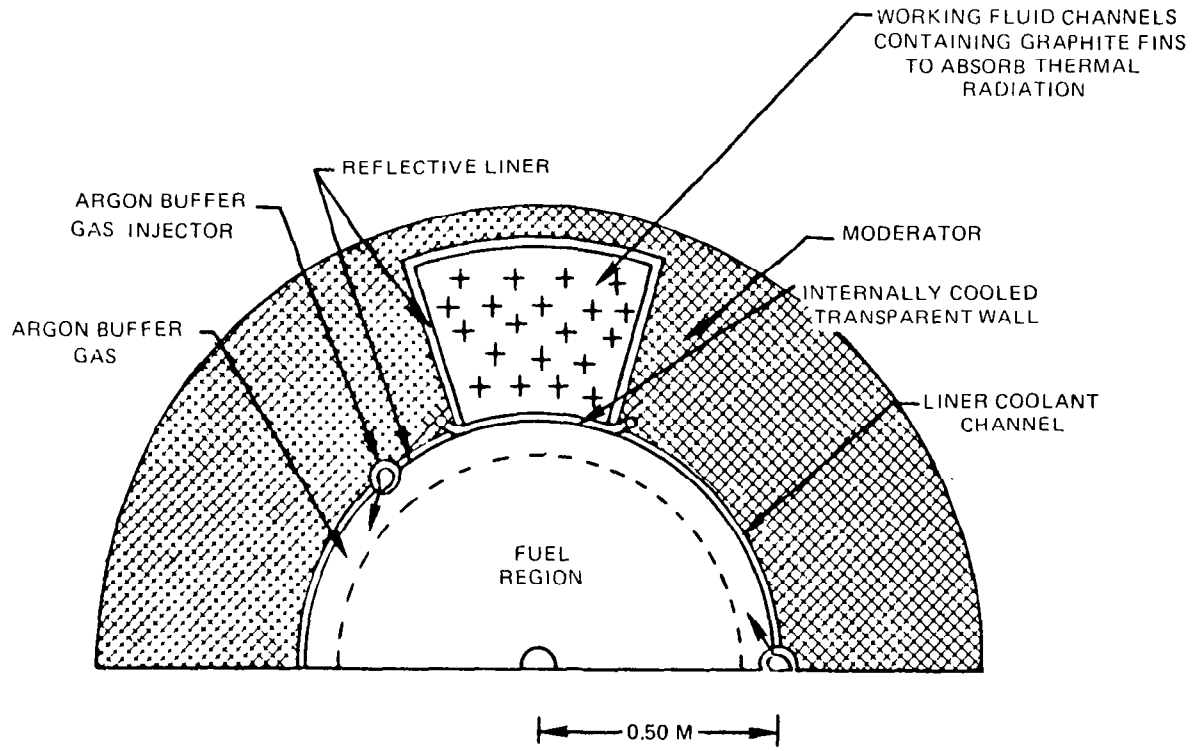


FIG. 1 DETAILS OF PLASMA CORE REACTOR UNIT CELL



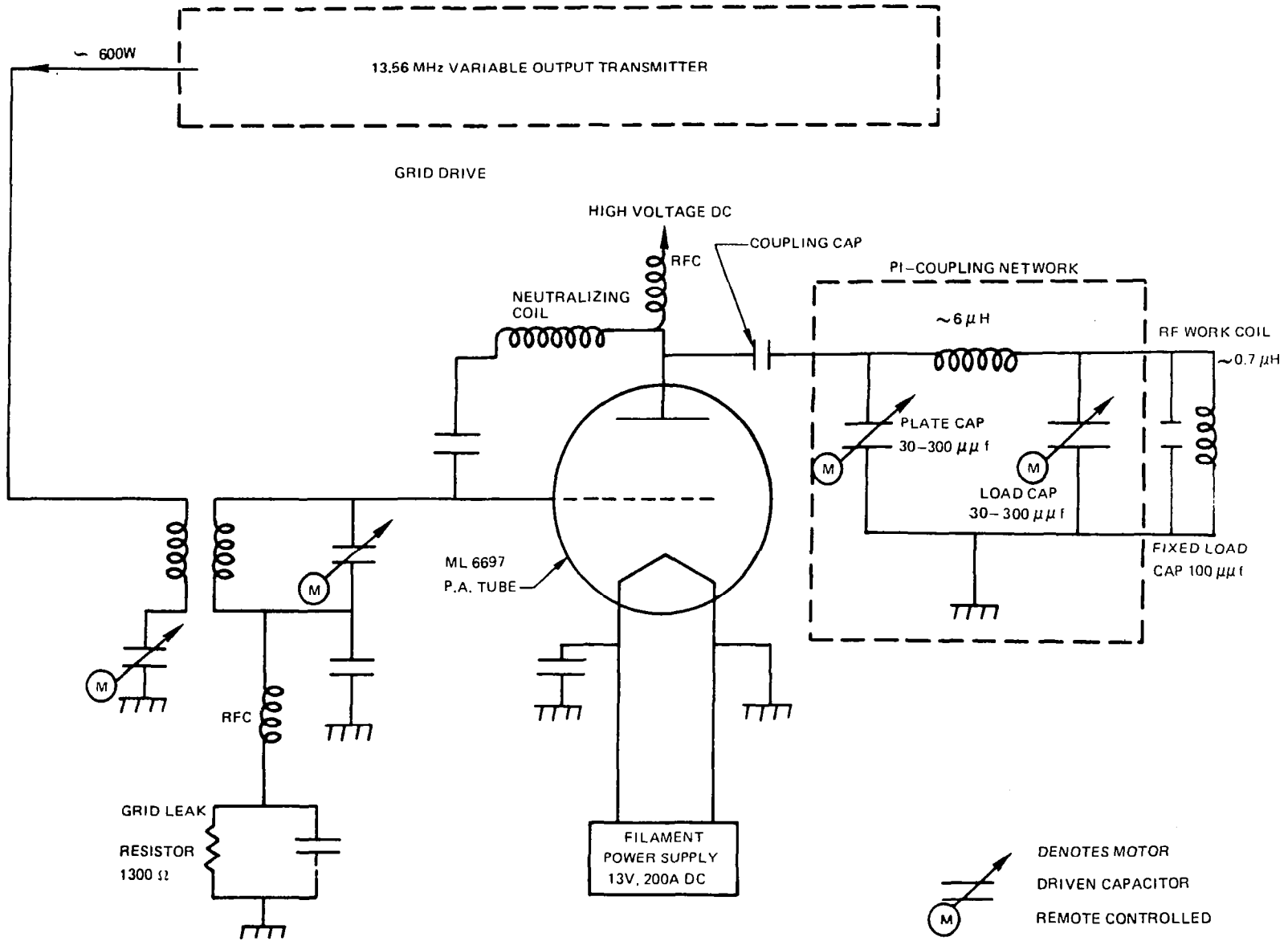


FIG. 2 SCHEMATIC DIAGRAM OF 80 KW RF INDUCTION HEATER

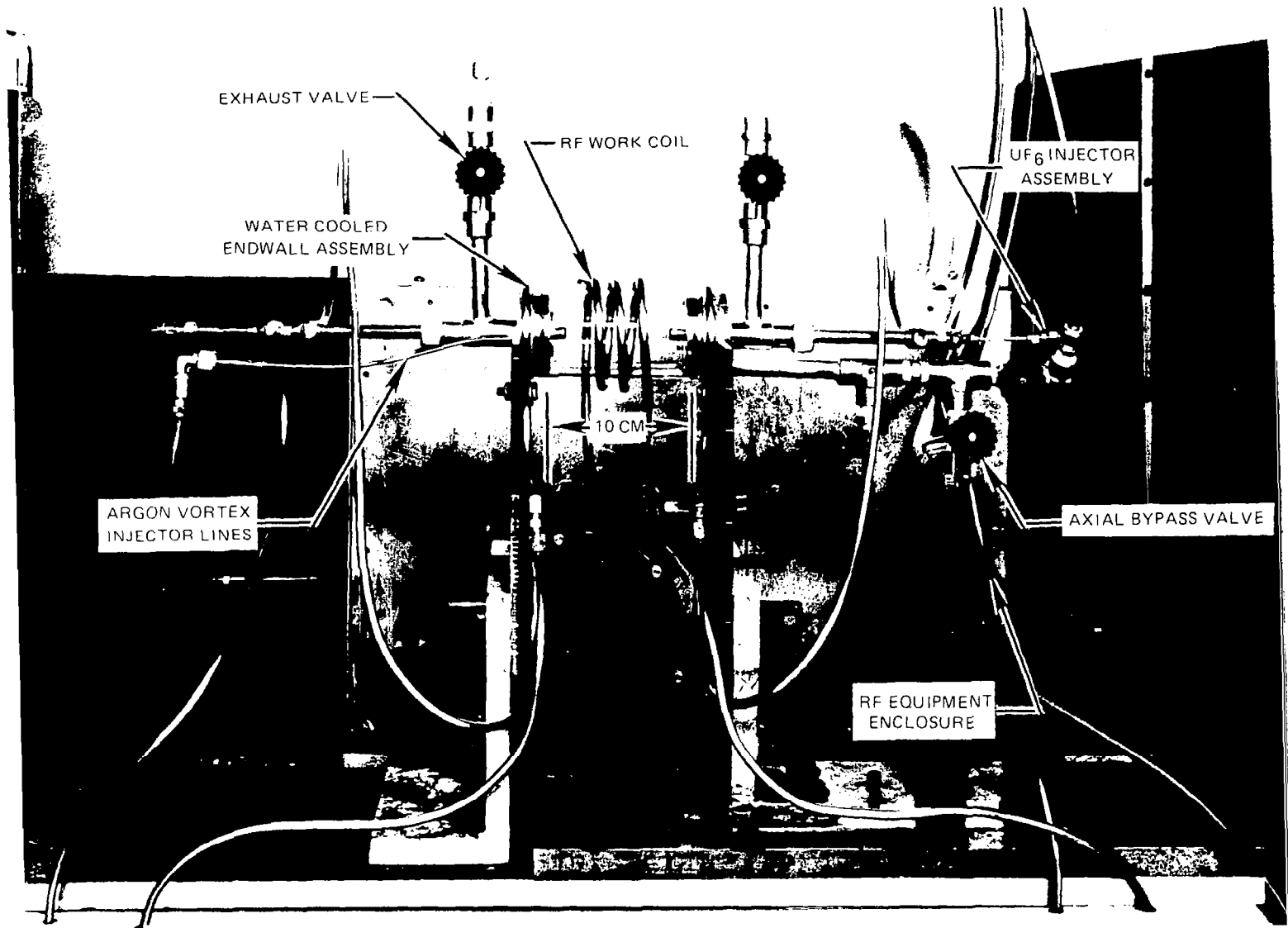


FIG. 3 PHOTOGRAPH OF TEST CHAMBER EMPLOYED IN EXPLORATORY TESTS IN 80 KW RF INDUCTION HEATER

FRONT ALUMINUM DOME WITH VIEW PORTS REMOVED FOR CLARITY  
TEST SECTION AXIAL DISTANCE - 10 CM

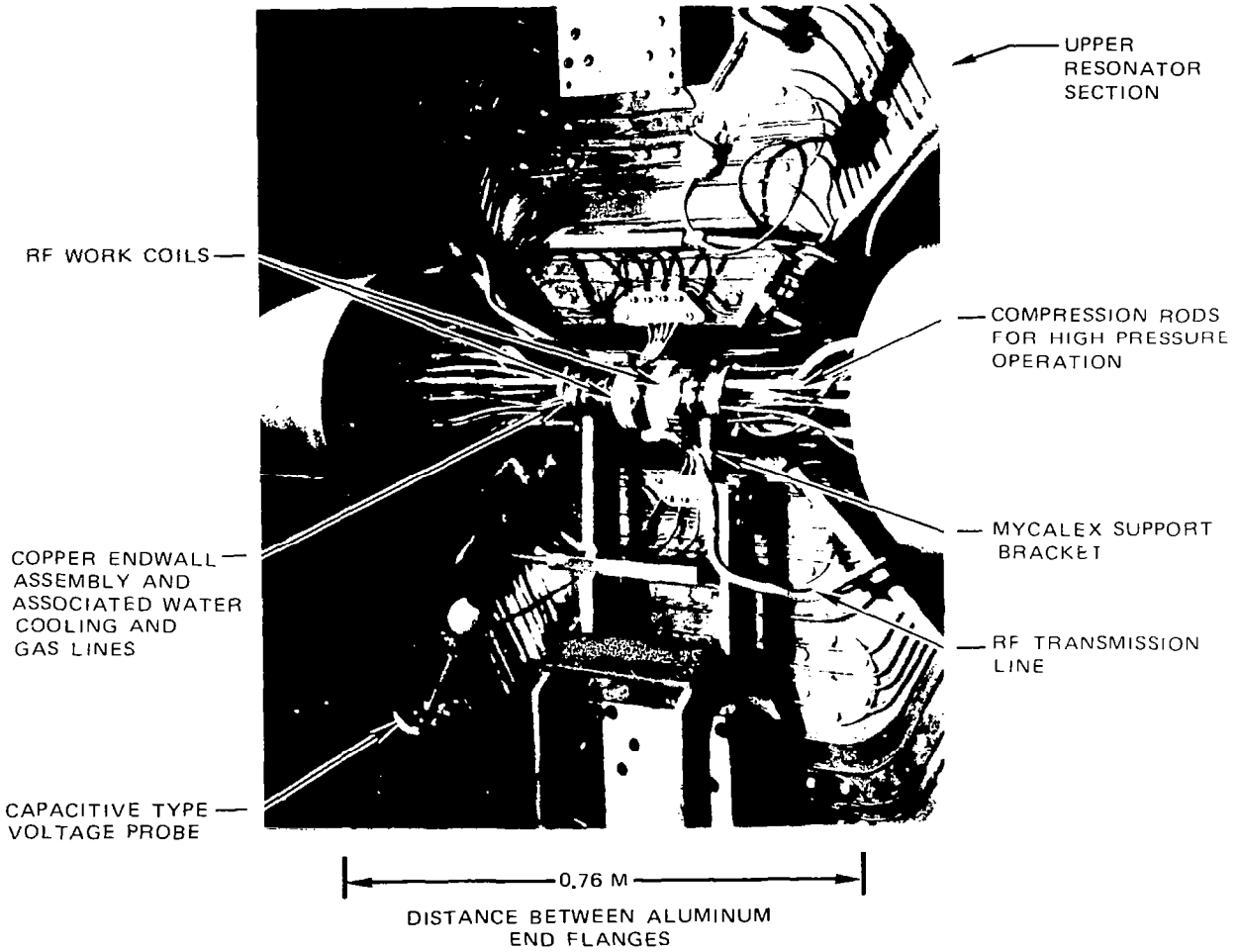


FIG. 4 PHOTOGRAPH OF TEST CHAMBER CONFIGURATION INSTALLED  
IN 1.2 MW RF INDUCTION HEATER

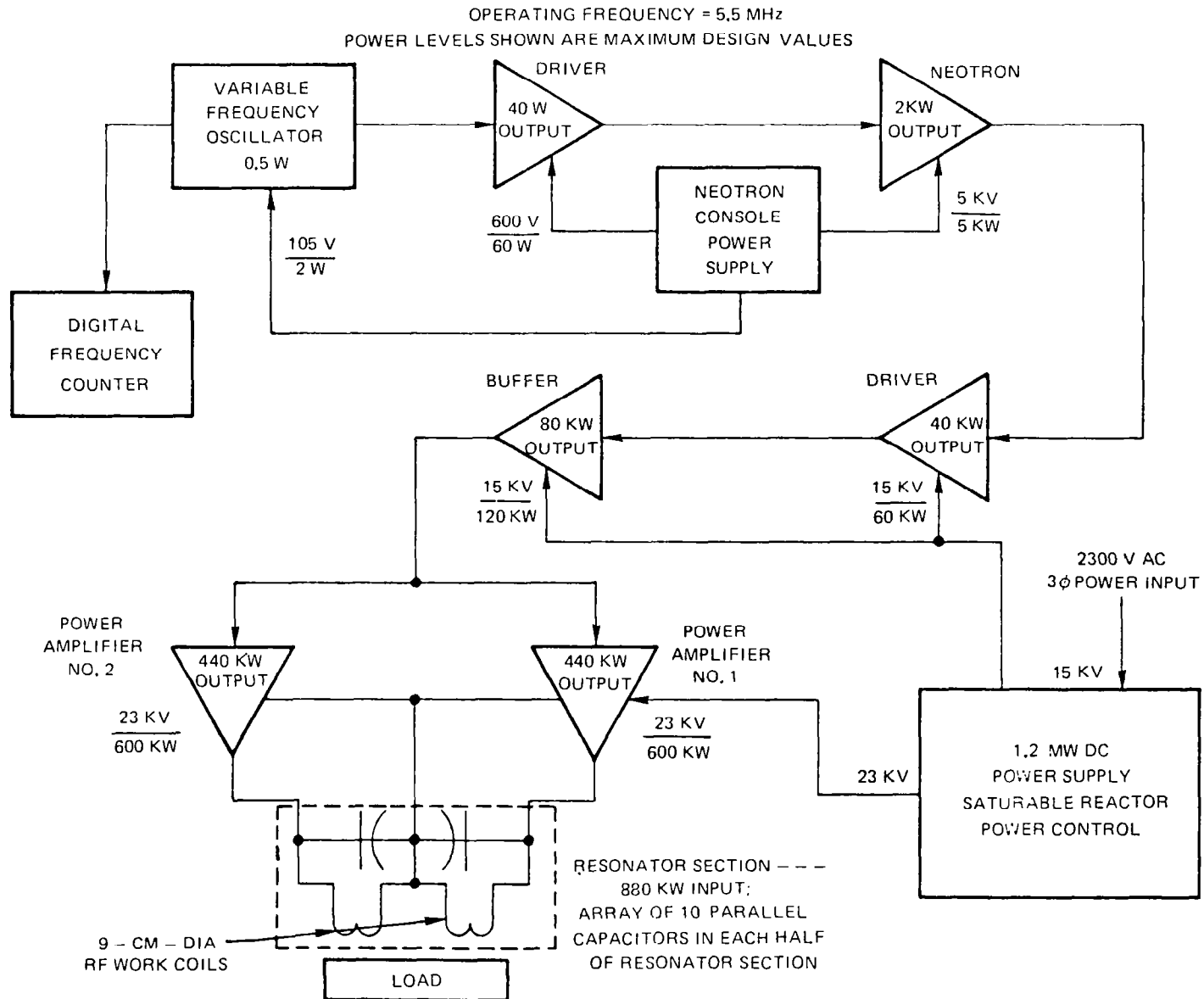
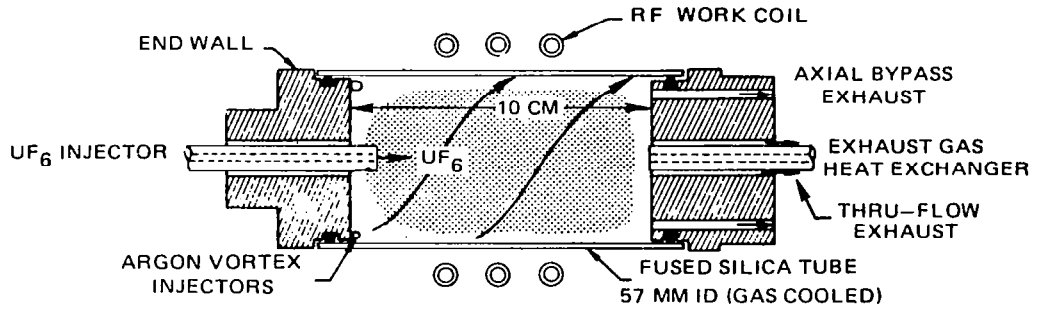
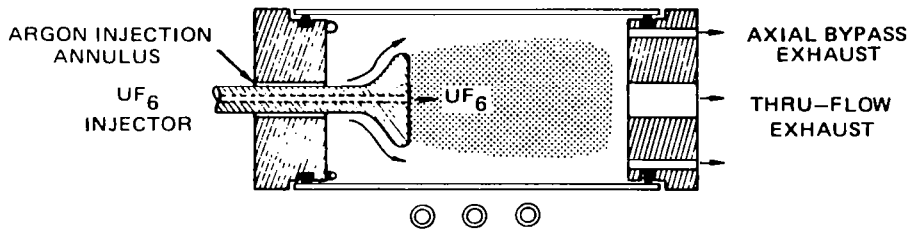


FIG. 5 BLOCK DIAGRAM OF UTRC 1.2 MW RF INDUCTION HEATER

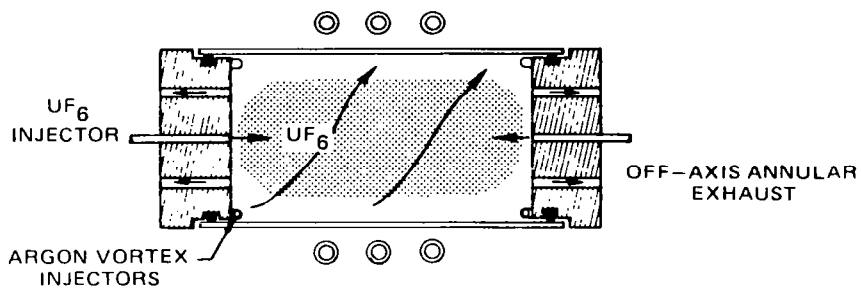
a) END WALL INJECTION WITH ON-AXIS THRU FLOW EXHAUST AND PROVISION FOR AXIAL BYPASS



b) END WALL INJECTION WITH BLUFF BODY STABILIZATION AND ON-AXIS THRU FLOW EXHAUST



c) END WALL INJECTION WITH OFF-AXIAL ANNULAR EXHAUST



d) PERIPHERAL WALL INJECTION

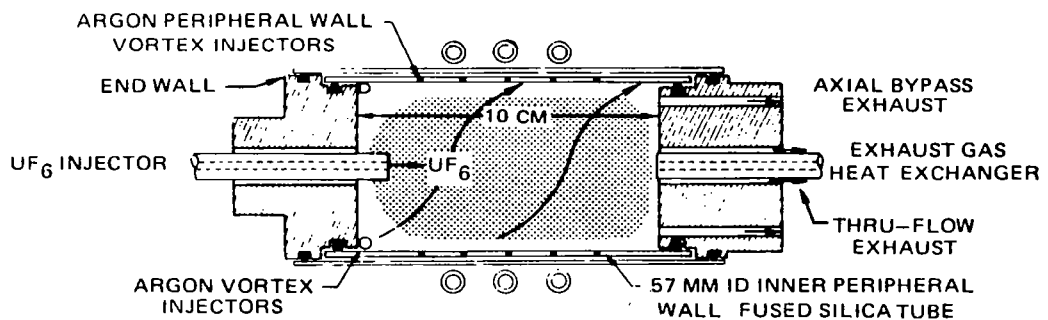
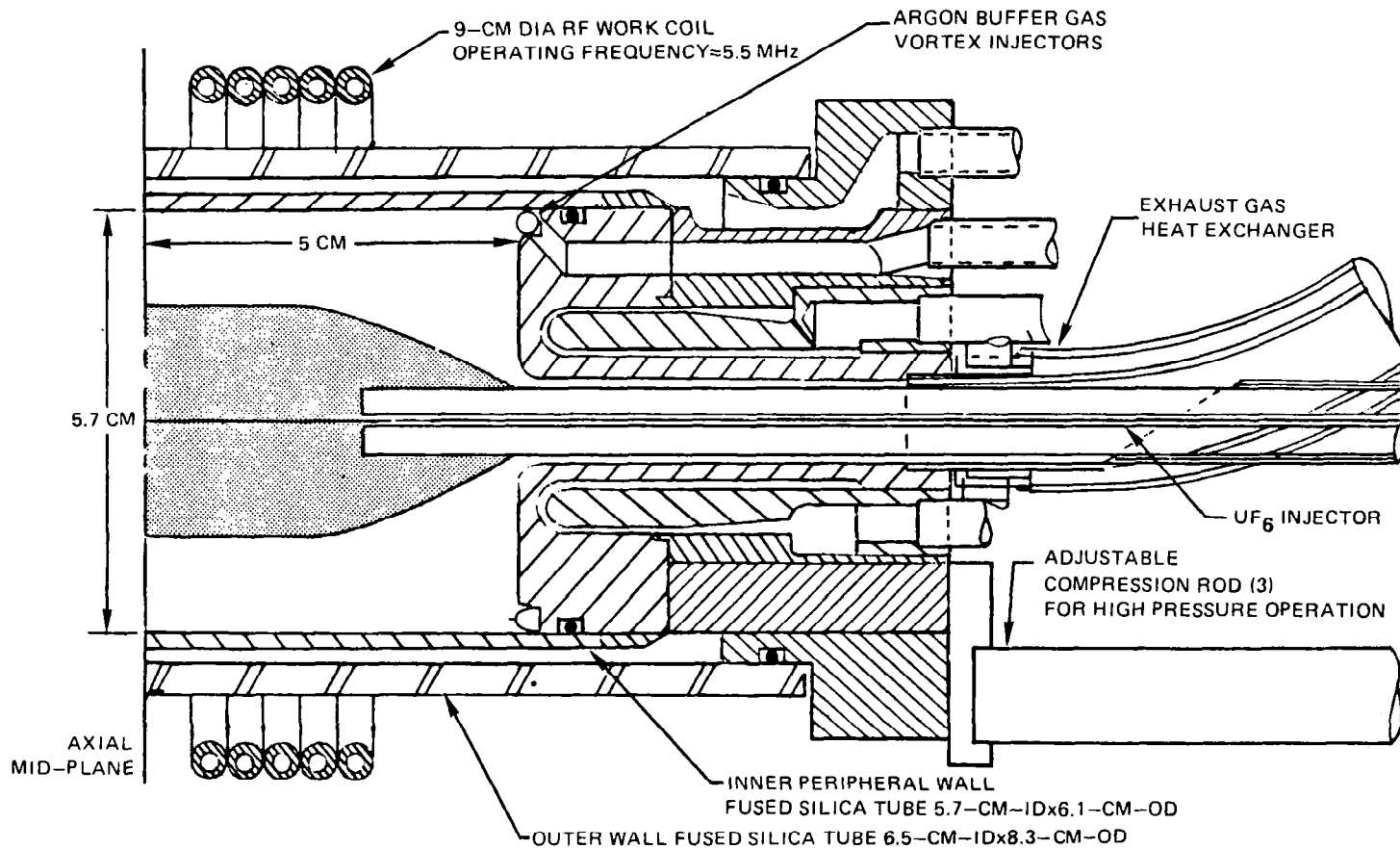


FIG. 6 SKETCH OF TEST CHAMBERS EMPLOYED IN 80 KW EXPLORATORY RF PLASMA TESTS WITH PURE  $UF_6$  INJECTION



OPERATING RANGE:

CHAMBER PRESSURE 1-12 ATM

RF DISCHARGE POWER 10-85 KW

ARGON BUFFER GAS FLOW RATE 1-10 G/S

DISCHARGE DIAMETER AT AXIAL MID-PLANE 1.5-3.5 CM.

FIG. 7 SKETCH OF TEST CHAMBER CONFIGURATION USED IN TESTS IN 1.2 MW RF INDUCTION HEATER USING PURE UF<sub>6</sub> INJECTION

DESIGN POINT FLOW RATE = 5 G/S

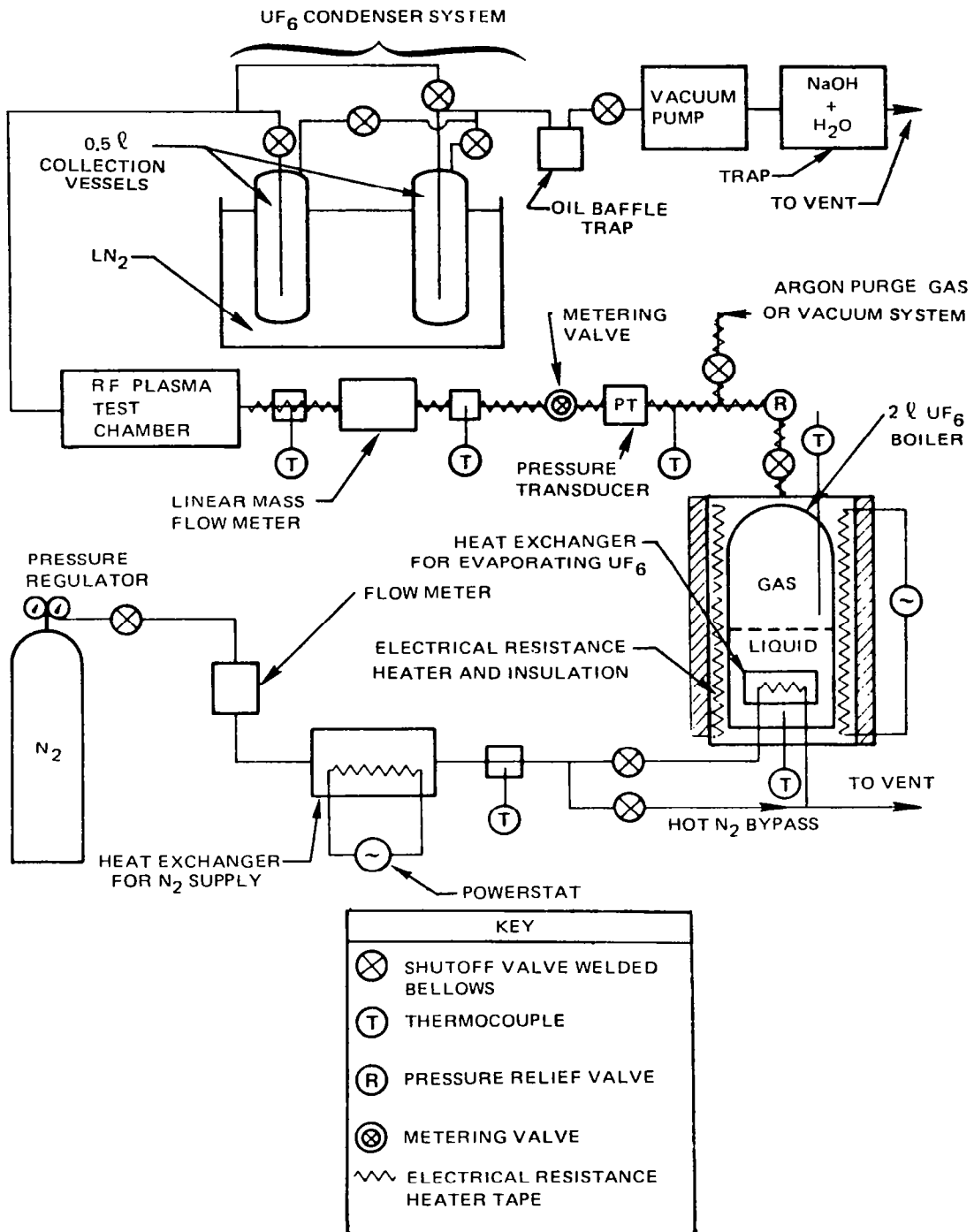


FIG. 8 SCHEMATIC DIAGRAM OF UF<sub>6</sub> TRANSFER SYSTEM

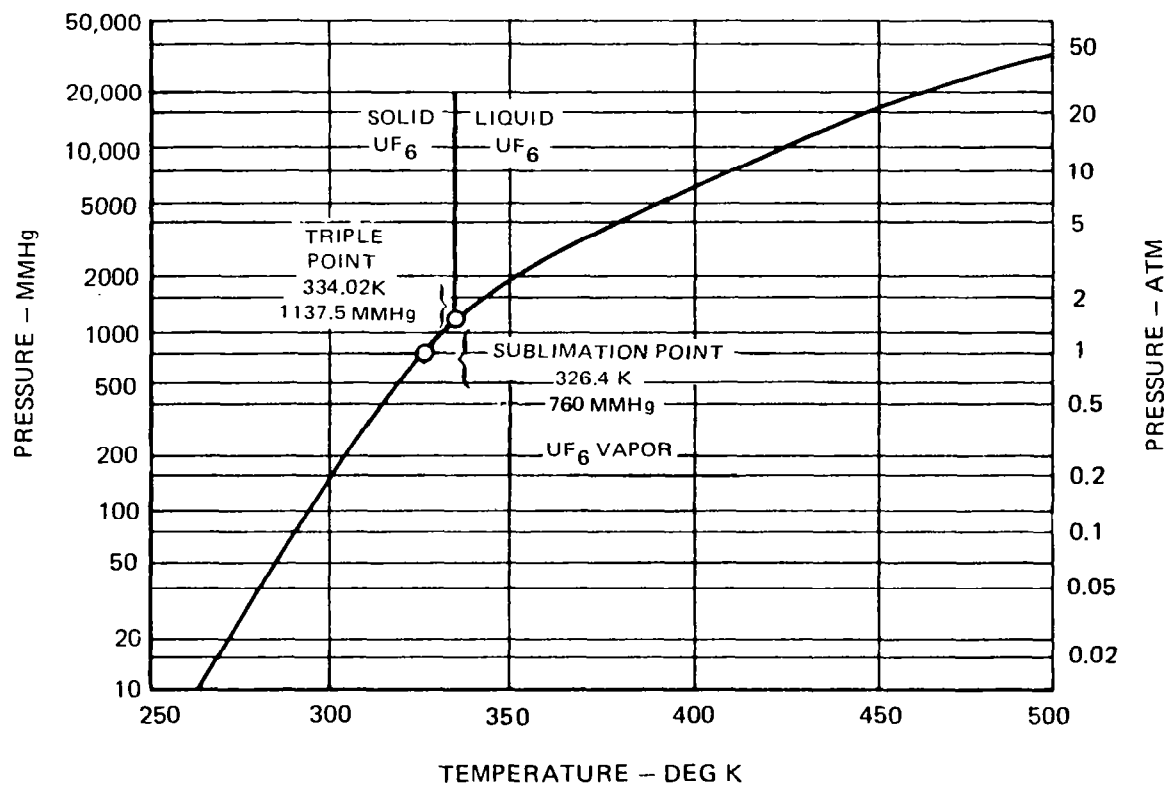
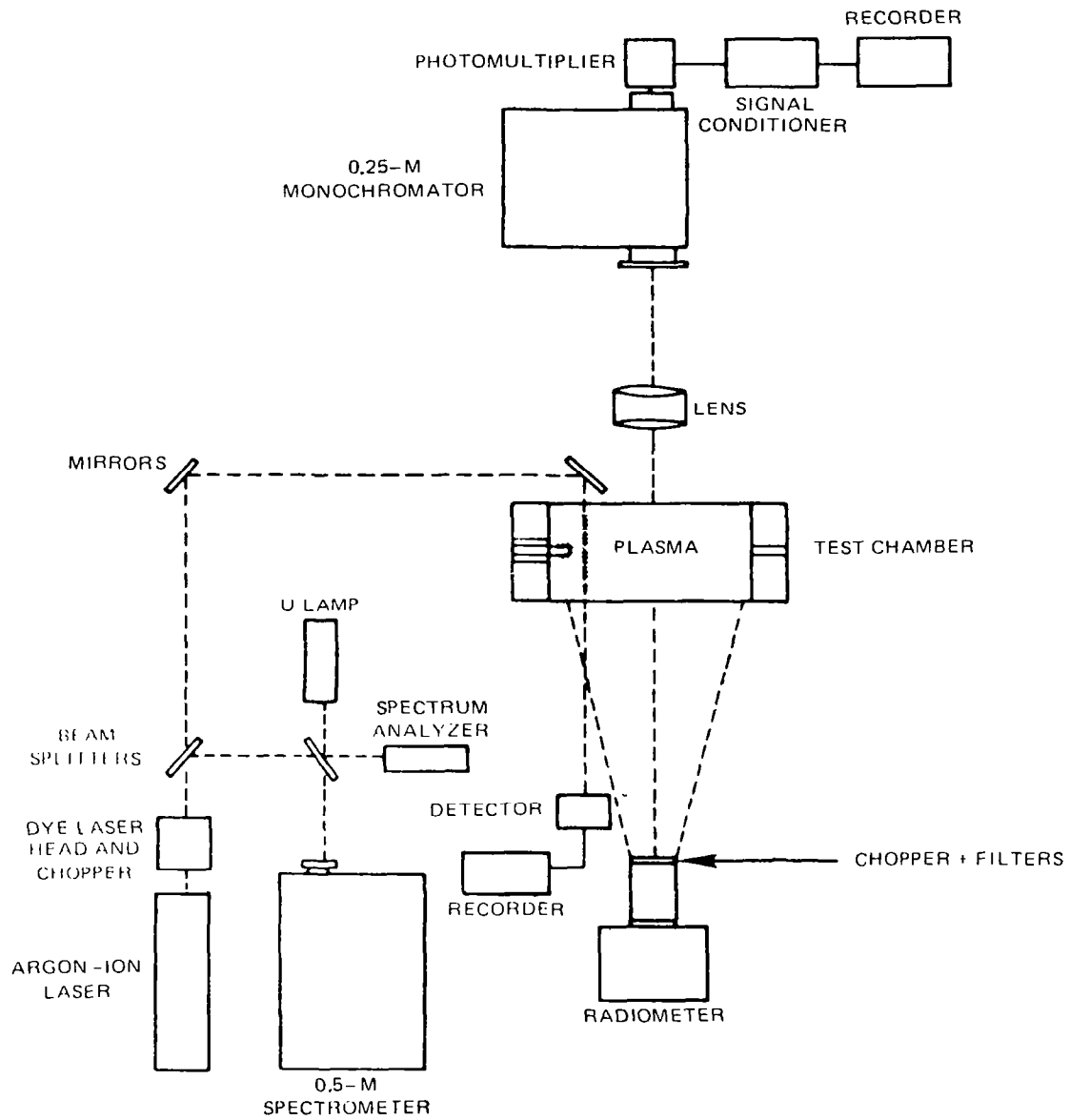


FIG. 9 VAPOR PRESSURE CURVE FOR URANIUM HEXAFLUORIDE





**FIG. 10 SCHEMATIC OF DIAGNOSTIC SYSTEMS  
USED IN EXPLORATORY RF PLASMA TESTS**

SEE FIG. 6(a) FOR SKETCH OF TEST CHAMBER FLOW CONFIGURATION  
 TESTS CONDUCTED IN 80 KW RF INDUCTION HEATER

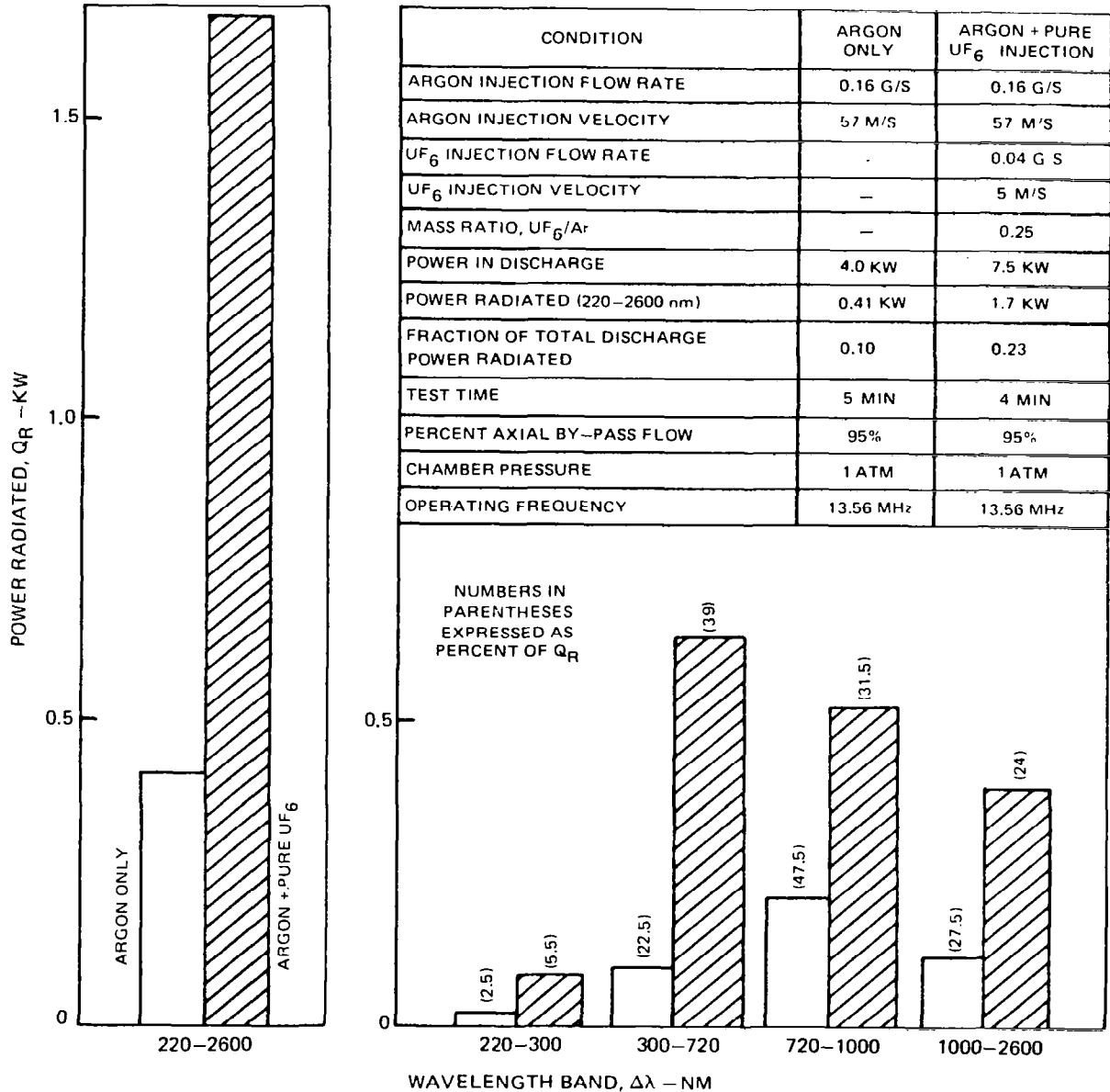


FIG. 11 TYPICAL OPERATING CONDITIONS AND RESULTS OF CORRESPONDING RADIATION MEASUREMENTS IN EXPLORATORY RF PLASMA TESTS WITH PURE UF<sub>6</sub> INJECTION

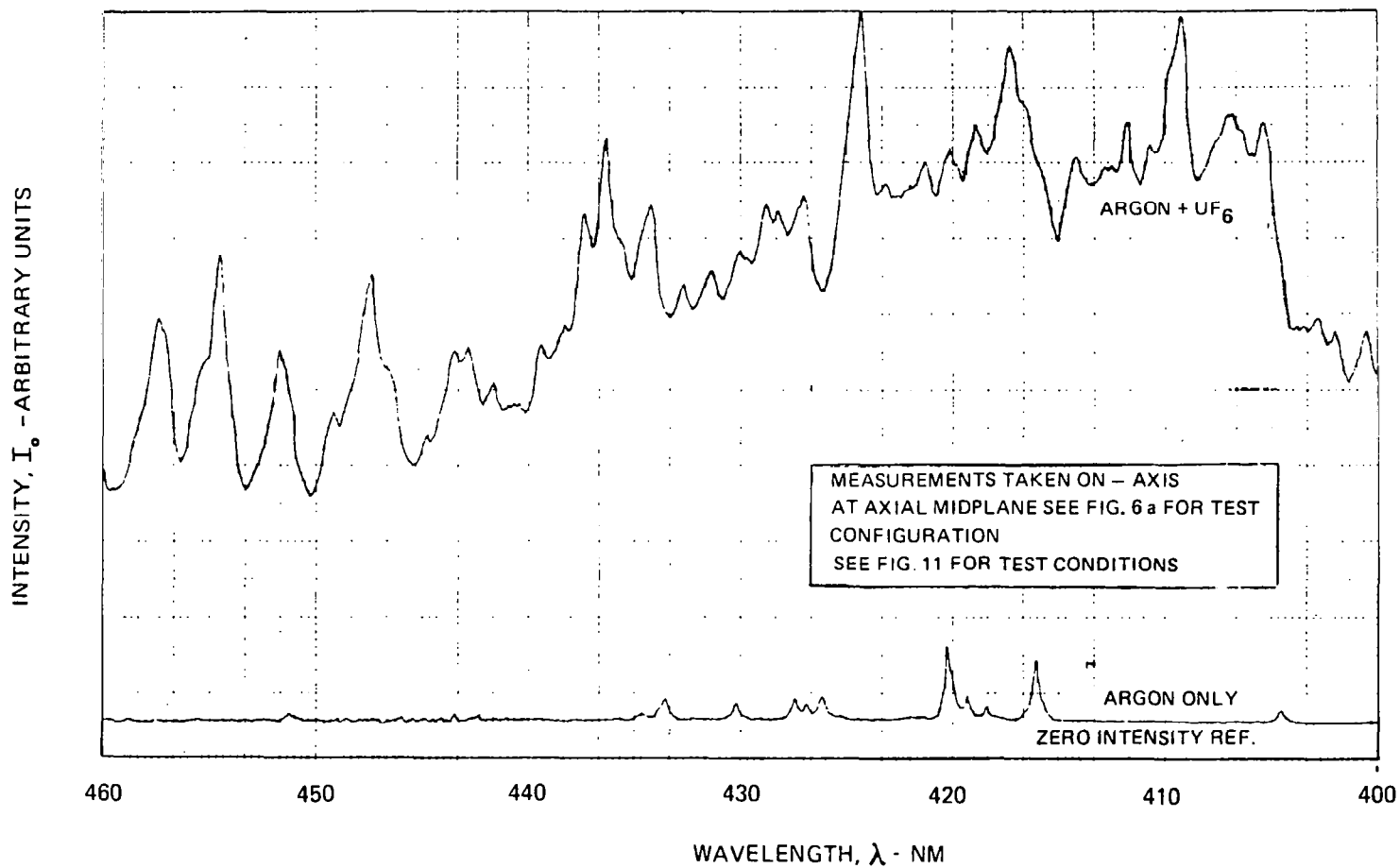


FIG. 12 RESULTS OF SPECTRAL EMISSION MEASUREMENTS FROM EXPLORATORY TESTS  
 WITH PURE UF<sub>6</sub> INJECTION

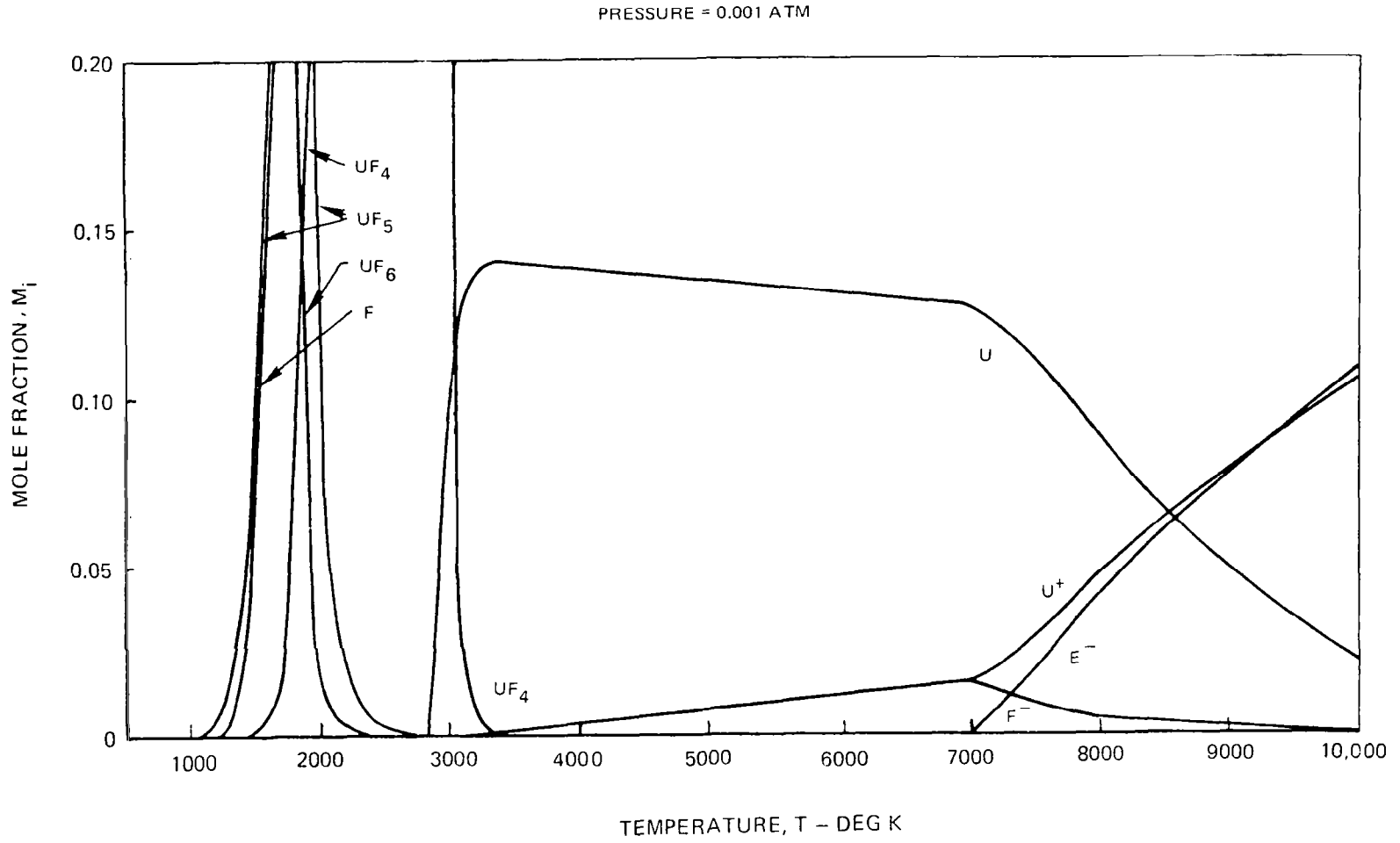


FIG. 13 EXAMPLE OF  $UF_6$  EQUILIBRIUM COMPOSITION DATA

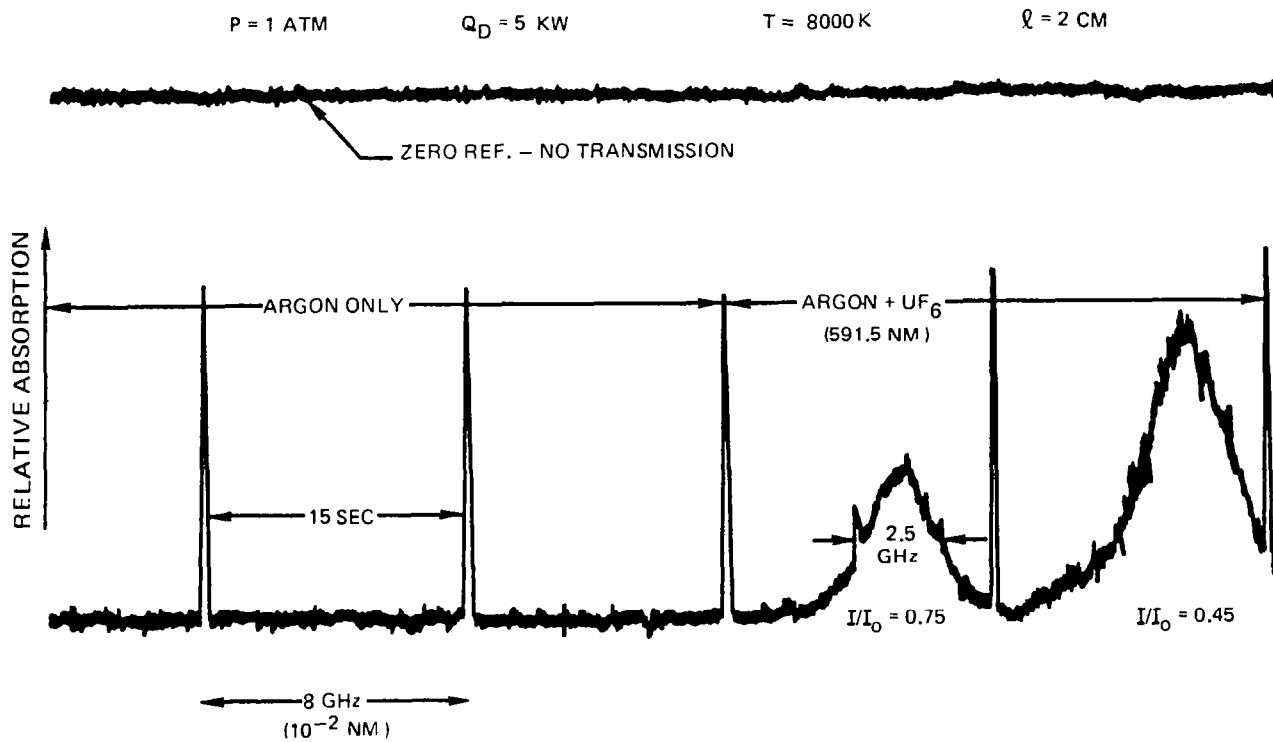


FIG. 14 EXAMPLE OF ABSORPTION MEASUREMENTS OBTAINED IN EXPLORATORY RF PLASMA TESTS

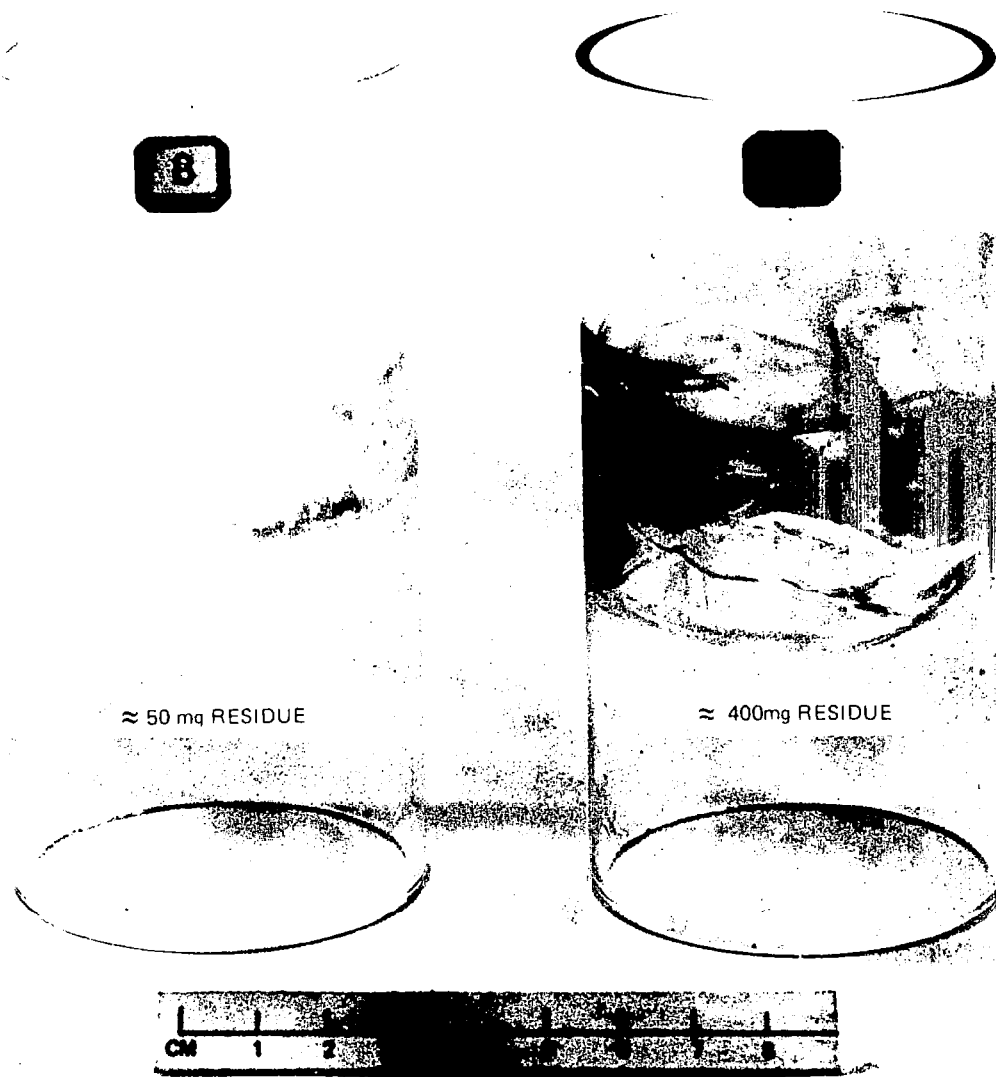


FIG. 15 PHOTOGRAPH OF FUSED-SILICA TUBES USED IN EXPLORATORY RF PLASMA TESTS WITH PURE  $UF_6$  INJECTION

SEE FIG. 7 FOR DETAILS OF TEST CONFIGURATION AND OPERATING RANGE

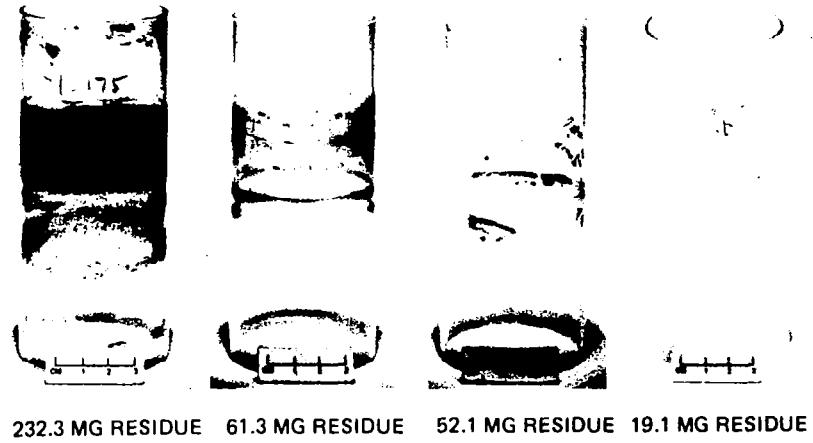
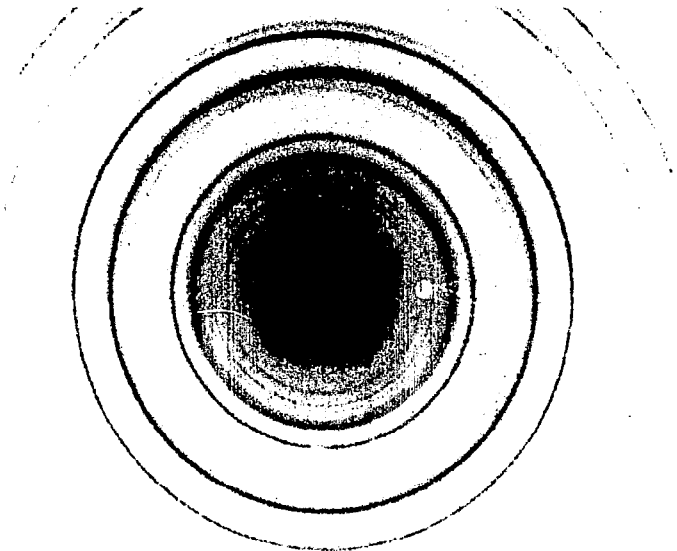


FIG. 16 PHOTOGRAPH OF FUSED - SILICA TUBES USED IN 1.2 MW RF PLASMA TESTS WITH PURE  $UF_6$  INJECTION

[UF<sub>4</sub>, UO<sub>2</sub>]



12-701

d	4.21	3.73	2.08	7.52	UF <sub>4</sub>						
I/I <sub>1</sub>	100	90	70	20	URANIUM (IV) FLUORIDE						
Rad. CuKα	λ 1.5418	Filter MONOCHR.	Di. 22.9cm	d Å	I/I <sub>1</sub>	hkl	d Å	I/I <sub>1</sub>	hkl		
Cut off 121/2A. I/I <sub>1</sub> VISUAL ESTIMATE						7.52	20	110	2.441	10	223
Ref. E. V. GARNER, UNITED KINGDOM ATOMIC ENERGY AUTHORITY, CAPEHURST, CHESHIRE, ENGLAND						6.63	23	111	2.121	40	602
S.G. MONOCLINIC S.G. C2/c (15)						5.41	10	020	2.109	20	042
a <sub>0</sub> 12.82 b <sub>0</sub> 10.74 c <sub>0</sub> 8.41 A 1.194 C 0.78?						5.17	20	200	2.095	40	404
α β 126°10' γ Z D <sub>1</sub>						4.213	100	021	2.079	70	241
Ref. ZACHARIASEN, ACTA CRYST., 2 393 (1949)						4.183	60	202	2.068	70	331
f <sub>a</sub> n w β f γ Sign						3.957	60	311	2.036	10	442
2V D n w β f γ Color						3.728	80	220	2.024	20	441
Ref.						3.555	60	312	2.001	60	
						3.274	40	130	1.986	40	INDEXED BY THE INSTITUTE OF PHYSICS AT UNIVERSITY COLLEGE, CARLISLE.
						3.299	60	222, 131	1.977	40	
						3.276	50	310			
						2.799	10	221			
						2.782	10	-			
						2.705	40	313			
						2.699	40	112			
						2.666	20	132			
						2.590	20	400			
						2.471	20	241			
						2.454	10	311			

5-0550

d	3.16	1.93	2.74	3.15	UO <sub>2</sub>					
I/I <sub>1</sub>	100	49	48	100	URANIUM DIOXIDE URANINITE					
Rad. Cu	λ 1.5405	Filter		d Å	I/I <sub>1</sub>	hkl	d Å	I/I <sub>1</sub>	hkl	
Di. Cut off						3.157	100	111		
I/I <sub>1</sub> d corr. abs.?						2.735	48	200		
Ref. SWANSON AND FUYAT, NBS CIRCULAR 539, Vol. II, 33 (1953)						1.934	49	220		
S.G. CUBIC S.G. O <sub>H</sub> - Fm3m						1.649	47	311		
a <sub>0</sub> 5.4682 b <sub>0</sub> c <sub>0</sub> A C						1.579	13	222		
α β γ Z 4						1.368	9	400		
Ref. ibid.						1.255	18	331		
						1.223	15	420		
						1.1163	13	422		
						1.0523	15	511		
f <sub>a</sub> n w β f γ Sign						0.9666	6	440		
2V D <sub>1</sub> 10.968mp Color						.9243	15	531		
Ref.						.9114	8	600		
						.8646	9	620		
SAMPLE FROM AEC. ACTUAL COMP. 1 UO <sub>2.08</sub> FROM URANIUM ANALYSIS AND OXYGEN BY DIFFERENCE.						.8339	7	533		
SPECT. ANALYSIS: < 0.006% EACH OF AL, CA, CU, FE, NA, SI; < 0.001% EACH OF BE, CR, MG, MN, NI, PB, SN.						.8243	7	622		
X-RAY PATTERN AT 26°C.										

FIG.17 EXAMPLE OF ELECTRON DIFFRACTION ANALYSIS

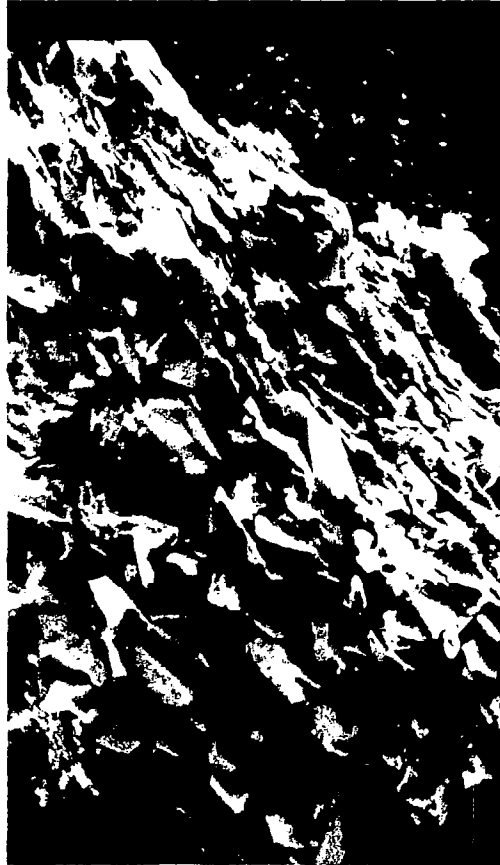


MAGNIFICATION : 800x

$\alpha\text{UO}_3, \text{U}_3\text{O}_8$



$\text{U}_4\text{O}_9, \text{UO}_2$



$\text{UF}_4$



FIG.18 PHOTOMICROGRAPHS OF RESIDUE WALL COATING FROM 1.2 MW  
RF PLASMA TESTS WITH PURE  $\text{UF}_6$  INJECTION

ALL SAMPLES SUBJECT TO COPPER  $k\alpha$  RADIATION IN A DEBYE CAMERA

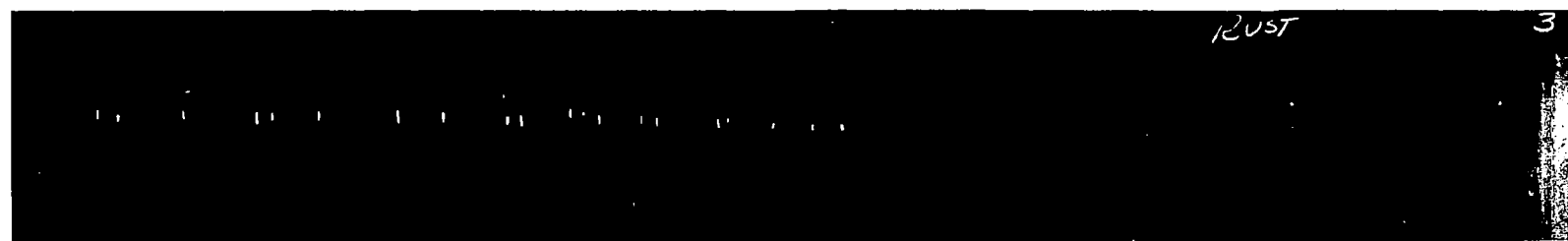
38



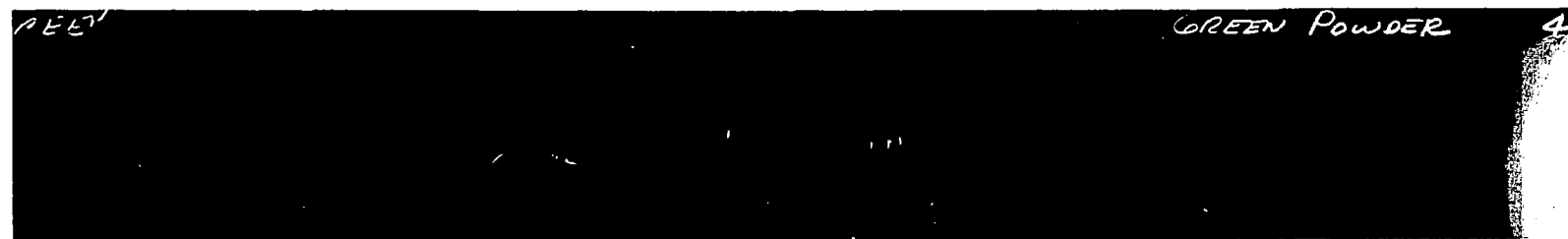
BLACK CHIP -  $\alpha\text{UO}_3, \text{U}_3\text{O}_8$



BLACK POWDER -  $\alpha\text{UO}_3, \text{U}_3\text{O}_8$



RUST POWDER -  $\text{UO}_2, \text{U}_4\text{O}_9$



GREEN POWDER -  $\text{UF}_4$

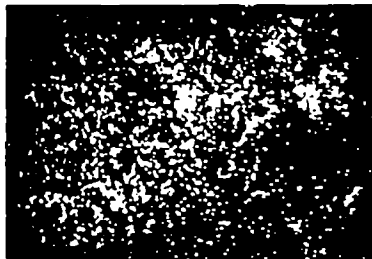
FIG. 19 EXAMPLE OF X-RAY DIFFRACTION PATTERNS OBTAINED FROM POST TEST ANALYSIS OF RESIDUE WALL COATING

MAGNIFICATION: 350x

a) URANIUM



b) FLUORINE



c) OXYGEN



FIG. 20 PHOTOGRAPH OF X-RAY DISTRIBUTION FOR U, F, AND O ON SAMPLE OF RESIDUE WALL COATING FROM POST TEST ANALYSIS

INSTRUMENT USED: IR SPECTROPHOTOMETER USED IN CONJUNCTION WITH 3x-BEAM CONDENSER AND  
SPECULAR REFLECTANCE ACCESSORY

PREPARATION: THIN WAFER KBr MATRIX

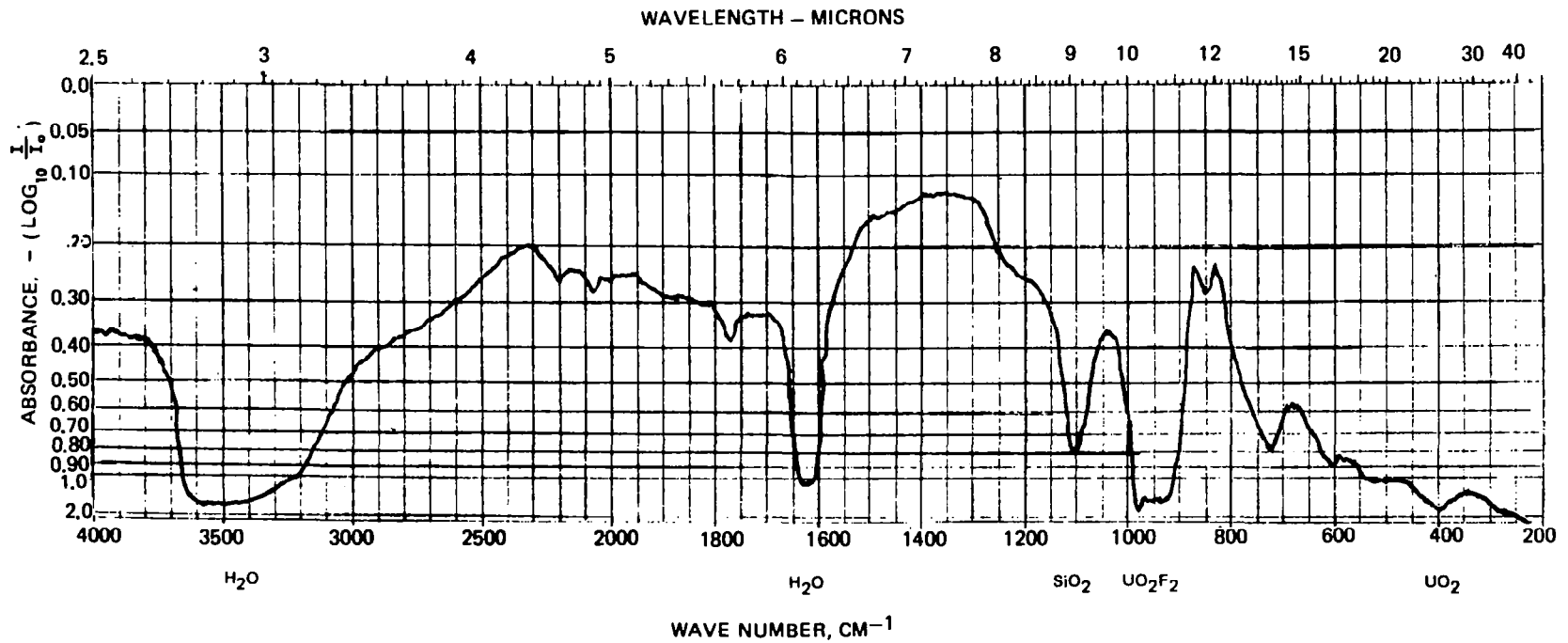


FIG. 21 EXAMPLE OF IR SPECTROPHOTOMETRY ABSORPTION MEASUREMENTS OBTAINED FROM  
POST TEST ANALYSIS OF RESIDUE WALL COATING

SEE FIG. 7 FOR SKETCH OF TEST CONFIGURATION USED IN TESTS  
 (LASER BEAM TRAVERSED ON-AXIS AT AXIAL MID-PLANE)  
 SEE FIG.10 FOR SCHEMATIC OF DIAGNOSTIC SYSTEM  
 (DYE LASER HEAD NOT USED IN THESE TESTS)

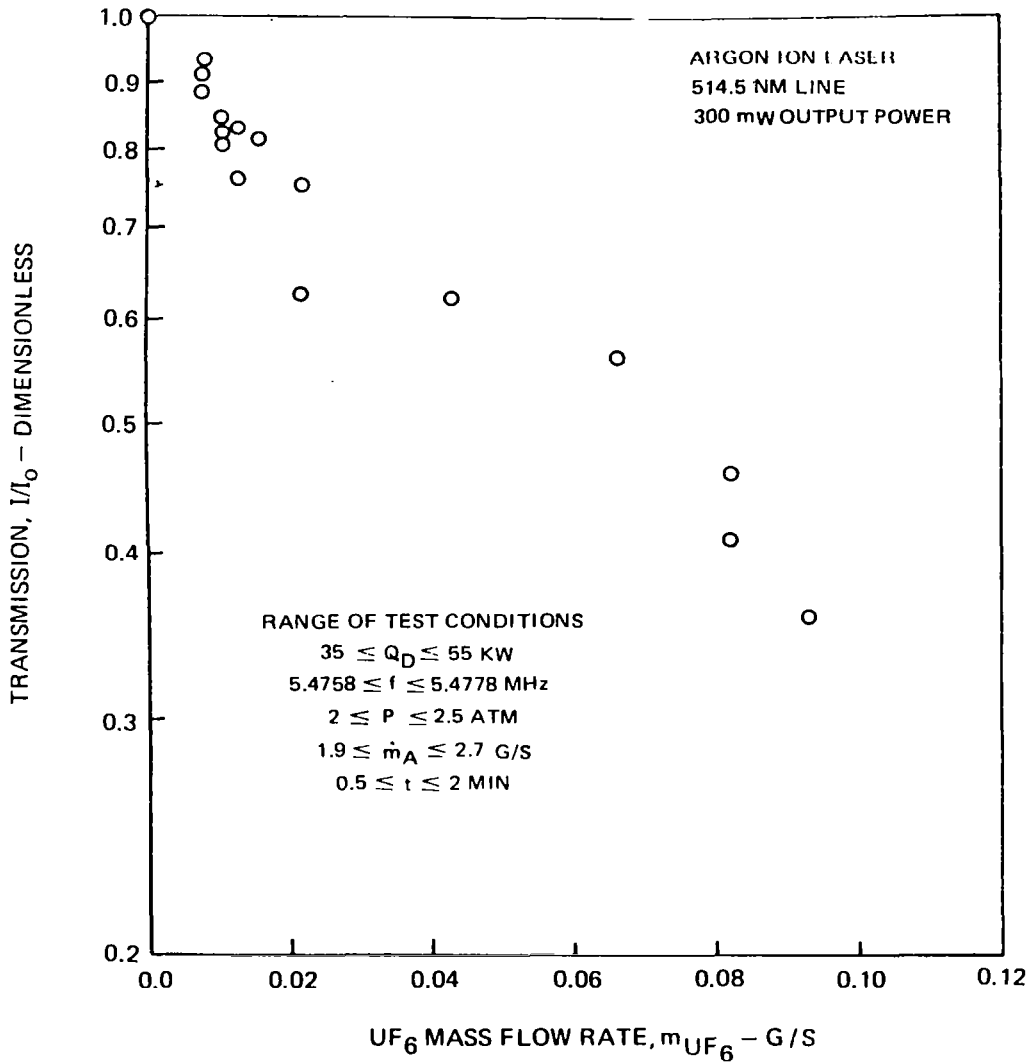


FIG. 22 EXAMPLE OF ABSORPTION MEASUREMENTS OBTAINED IN 1.2 MW RF PLASMA TEST WITH PURE UF<sub>6</sub> INJECTION

$P = 2.4 \text{ ATM}$     $Q_D = 52 \text{ KW}$     $f = 5.4778 \text{ MHz}$     $d = 2.9 \text{ CM}$

$\dot{m}_{\text{Ar}} = 2.2 \text{ G/S}$     $\dot{m}_{\text{UF}_6} = 0.09 \text{ G/S}$



10 CM

FIG. 23 PHOTOGRAPH OF RF ARGON PLASMA IN 1.2 MW RF INDUCTION HEATER TEST CHAMBER WITH PURE  $\text{UF}_6$  INJECTION